



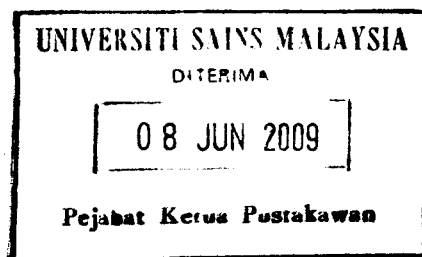
UNIVERSITI SAINS MALAYSIA

**PEJABAT PENGURUSAN DAN KREATIVITI PENYELIDIKAN**

RESEARCH CREATIVITY AND MANAGEMENT OFFICE

Tarikh: 27 Mei 2009

Profesor Dr. Rofina Yasmin Othman  
Setiausaha Bahagian  
Bahagian Bioteknologi Kebangsaan (BIOTEK)  
Kementerian Sains, Teknologi & Inovasi Malaysia  
Aras 4, Blok C4, Kompleks C  
Pusat Pentadbiran Kerajaan Persekutuan  
62662, PUTRAJAYA



Puan,

**LAPORAN AKHIR PROJEK IRPA RANCANGAN MALAYSIA KE-8 KATEGORI 'PR'**

Dengan hormatnya perkara di atas dirujuk.

2. Sehubungan dengan ini disertakan bersama sepuluh (10) laporan akhir bagi projek IRPA RMKe8 Kategori 'PR' bertajuk seperti berikut:-

Bil	No. Projek	Tajuk Projek	Penyelidik
1.	06-02-05-1021 PR0018/08-01	Understanding Individual Variations in Drug Responses: Development of Rapid Assays for CYP and NAT2 Genotyping	Teh Lay Kek
2.	06-02-05-1013 PR0018/08-02	A Study of Structure Function Relationship of Cytochromes P450 (CYP) and Their Involvement in Drug-Drug, Drug-Food and Drug-Herb Interactions	Profesor Rusli Ismail
3.	06-02-05-1014 PR0018/08-03	Understanding Individual Variations in Drug Responses: Genetic Epidemiology of Drug Metabolising Enzymes CYP2D6, CYP2C9, CYP2C19 and NAT2	Prof. Madya Tan Soo Choon
4.	06-02-05-1015 PR0018/08-04	Value Added Therapeutic Drug Monitoring: Application of Pharmacogenomic in the Management of Mental Illness	Profesor Mohd Razali Salleh
5.	06-02-05-1016 PR0018/08-05	Genetic Polymorphisms of CYP2D6 and Beta-2 Receptor: A Clinical Study with Metoprolol	Profesor Sharif Mahsufi Mansor
6.	06-02-05-1017 PR0018/08-06	Understanding Gene Defects in Drug Dependence	Prof. Madya Foong Kin
7.	06-02-05-1018 PR0018/08-07	Metoprolol-Ticlopidine Interaction: An Investigation of a Novel Clinical Application	Tariq Razak

18/06/09  
HAR, SRMS,  
SFM.

**CANSELORI**

11800 USM, Pulau Pinang, Malaysia

Tel : (6)04-653 3888 ext.2725 / 3895 / 3178 / 3194 / 3989 / 3988; Fax : (6)04-656 6466 / (6)04-656 8470 / (6)04-6532345

E-mail : dvc\_rd@notes.usm.my

8.	06-02-05-1019 PR0018/08-08	Human Acetyltransferase Polymorphisms: A Pharmacogenomic and Pharmacokinetic Study of Isoniazid in Tuberculosis	Profesor Yuen Kah Hay
9.	06-02-05-1027 PR0024/09-01	Identification on Infective Agents Associated with Cervical Cancer Among Women and Their Sexual Partners Using Molecular Technology	Profesor Nor Hayati Othman
10.	06-02-05-0000 PR0024/09	Determination of the Role of the Biological Factors (Angiogenesis, E-Cadherin, Telomerase and ILFG-R) in the Prognosis of the Cancer Cervix	Profesor Nor Hayati Othman/Prof. Madya M Madhavan

Sekian, untuk tindakan puan selanjutnya.

Terima kasih.

“BERKHIDMAT UNTUK NEGARA”  
‘Memastikan Kelestarian Hari Esok’

Yang menjalankan tugas,



**(MUHAMAD NIZAM SAAD)**

Pegawai Sains

Pejabat Pengurusan & Kreativiti Penyelidikan

Bahagian Penyelidikan & Inovasi

s.k. Profesor Nor Hayati Othman  
Dekan Penyelidikan  
Pelantar Sains Klinikal  
d/a Pejabat Pelantar Penyelidikan  
Universiti Sains Malaysia  
Kampus Kesihatan

Profesor Rusli Ismail  
Timbalan Pengarah  
(Penyelidikan & Siswazah)  
Institut Penyelidikan dan Perubatan Molekul (INFORMM)  
Universiti Sains Malaysia

Profesor Sharif Mahsufi Mansor  
Pengarah  
Pusat Penyelidikan Dadah & Ubat-Ubatan  
Universiti Sains Malaysia

Profesor Mohd Razali Salleh  
Pusat Pengajian Sains Perubatan  
Universiti Sains Malaysia  
Kampus Kesihatan

Profesor Yuen Kah Hay  
Pusat Pengajian Sains Farmasi  
Universiti Sains Malaysia

Prof. Madya Foong Kin  
Pusat Racun Negara  
Universiti Sains Malaysia

Prof. Madya Tan Soo Choon  
Pusat Kawalan Doping  
Universiti Sains Malaysia



Encik Mohd Pisol Ghadzali  
Ketua Pustakawan  
Perpustakaan Hamzah Sendut  
Universiti Sains Malaysia



*Disertakan satu salinan laporan untuk  
simpanan Perpustakaan*

# Surface Effects on Switching in Ferroelectric Films

Lye-Hock Ong<sup>\*</sup>, Ahmad Musleh, and Junaidah Osman

*School of Physics, Universiti Sains Malaysia, 11800 USM, Penang, Malaysia.*

**Abstract:** Surface effects on switching behaviours of ferroelectric (FE) films are elucidated by using the Landau Devonshire (LD) free energy expression. The well-known parameter,  $\delta$ , the extrapolation length, introduced in the LD free energy expression strongly influences the switching behaviours in FE films. Polarization at the surface can either be suppressed when  $\delta$  is positive or be enhanced when  $\delta$  is negative. We have discovered that the delay in switching at the centre relative to switching near the surfaces is more remarkable in the case of  $\delta = 0$  than the non-zero  $\delta$  cases, as the film thickness increases. It is also found that the reversals of dipole moments at the centre and near the surface, by the applied field, take place almost together in FE thin films of non-zero  $\delta$ . The results we obtained have shown that the surface extrapolation length  $\delta$  also influences the coercive field and critical thickness of FE films.

**Keyword:** Landau Theory, polarization reversal, extrapolation length.

**PACS Number:** 77.80.Fm.

## INTRODUCTION

Polarization reversal in ferroelectric (FE) materials has been an important area of study in ferroelectricity for a long time since some significant measurements on switching behaviours of FE crystals have been made by Merz and other workers [1, 2] about half a century ago. The interest in this research area has further extended to FE thin films; and the interest has not waned even up to these days because of the advancement in thin film fabrication technology, where higher quality and more reliable FE thin films can be fabricated; thus making applications of FE thin films in microelectronic devices and memories [3 – 5] more reliable. More current theoretical and experimental elucidations in polarization reversal in FE thin films are focused more on phenomena related to effects of size and surface in thin films on switching time and coercive field [6 – 10]. From the literature, on theoretical studies, several models based on a Landau-typed phase transition have given well explanations on switching behaviours of mesoscopic ferroelectric structures [7, 9]; and some of the predictions concerning size and surface effects on switching behaviours by Landau-typed models agree well with experimental observations. However, there still lacks detailed understanding of surface effects on FE films under the applied electric field, which is a very important portion of knowledge toward the overall understanding on the behaviours of polarization reversal in the films as a whole. In this paper, we adopt the Tilley-Zeks model of Landau Devonshire (LD) free energy expansion to study the effect of surface conditions under the applied electric field on a one dimensional FE film. With this framework, we present the results of switching behaviours of FE film with zero and non-zero values of  $\delta$  as surface conditions.

<sup>\*</sup>Corresponding author. E-mail address: onghl@usm.my

## THEORETICAL MODEL

A symmetric second-order FE thin film of thickness  $L$  in which the polarization and related dielectric quantities vary as a function of  $z$  is considered. The film thickness considered is much smaller than the lateral dimension, thus depolarization effects can be neglected. In our case, the film thickness extends from one surface with  $z = -L/2$  to another with  $z = +L/2$ ; and the effects due to surfaces are governed by an extrapolation length  $\delta$  [11]; where  $\delta$  can be positive or negative. For positive value of  $\delta$ , polarization is enhanced at the film surfaces and the reversed is true for negative  $\delta$ . Usual LD model used in elucidation of dynamic properties of FE films considers the effect of applied electric field  $E$  to the film without the surface potential term [10, 12]. However, it has been proposed by Ishibashi *et al.* [13] that the surface potential term due to the effect of electric field has been included in the free energy expression. Since the surface thickness in the continuum model is zero, we have the opinion that the surface potential due to electric field may not be necessary to be considered in the free energy as many researchers have. With these conditions stated, the LD free energy per unit area of the film can be defined:

$$\frac{F}{S} = \int_{-L/2}^{L/2} f(P, P') dz + \frac{C}{2\delta\epsilon_0} (P_-^2 + P_+^2) \quad (1)$$

where  $f(P, P') = \frac{1}{2\epsilon_0} AP^2 + \frac{1}{4\epsilon_0^2} BP^4 - EP + \frac{1}{2\epsilon_0} CP'^2$ ,  $P' = \frac{dP}{dz}$ , and  $P_{+,-} = P\left(\pm \frac{L}{2}\right)$ . The parameters  $B$  and  $C$  are the usual second-order Landau coefficients, while  $A = \alpha(T - T_0)$  with  $\alpha$  is the inverse Curie constant and  $T_0$  is the bulk critical temperature. Minimization of Eq. 1 by variational method shows that the polarization satisfies the Euler Lagrange (EL) equation

$$\frac{A}{\epsilon_0} P + \frac{B}{\epsilon_0^2} P^3 - E - \frac{C}{\epsilon_0} \frac{d^2 P}{dz^2} = 0 \quad (2)$$

with the following boundary conditions:

$$\frac{dP}{dz} = \pm \frac{P}{\delta} \quad \text{at} \quad z = \pm L/2. \quad (3)$$

For the purpose of numerical calculations, Eq. 2 and Eq. 3 are scaled to dimensionless units in the normal way [16], and we have

$$(t-1)p + p^3 - \frac{2}{3\sqrt{3}} e - \frac{d^2 p}{d\zeta^2} = 0 \quad (4)$$

$$\frac{dp}{d\zeta} = \pm \frac{p}{d} \quad \text{at} \quad \zeta = \pm l/2 \quad (5)$$

where  $p = P/(\epsilon_0 \alpha T_0 / B)^{1/2}$ ;  $t = T/T_0$ ;  $e = E/(\alpha^3 T_0^3 / \epsilon_0 B)^{1/2}$ ;  $\zeta = z/\xi_0$ ,  $\xi_0^2 = C/\alpha T_0$ ;  $l = L/\xi_0$  and  $d = \delta/\xi_0$ . The length scales  $L$ ,  $d$  and  $\lambda$  are usually scaled according to  $\xi_0$ , the characteristic length of the material [10, 11] and it can be related to the thickness of domain wall.

## NUMERICAL CALCULATIONS

To discuss the dynamics of polarization reversal in the film, the Landau-Khalatnikov (LK) equation of motion is applied. As a consequence of omitting the kinetic term for low frequency studies, the dimensionless LK equation, following the scaling mentioned above, can be written as follow:

$$\frac{dp}{d\tau} = -(t-1)p - p^3 + \left(\frac{d^2P}{d\zeta^2}\right) + \frac{2}{3\sqrt{3}}e \quad (6)$$

where  $\frac{dp}{d\tau}$  is the dimensionless switching current and  $\tau$  ( $\tau = t' / \frac{\alpha T}{\epsilon C}$ ;  $t'$  is the time in real unit) is the reduced time. Polarizations at the film surfaces are influenced by the extrapolation length  $\delta$  during switching. Numerical process in simulation of switching profiles in various cases of surface conditions requires a static polarization profile as initial value for the LK equation and the exact solution from equations Eq. 2 and Eq. 3 has been obtained by Ong *et al.* [11]. When an electric field  $e$  ( $e > e_{cf}$ ) is applied, LK equation in Eq. 6 is used to simulate the profiles of polarization during switching.

The applied electric field used in the simulation takes the form of step function in reduced units as

$$e = e_0 \theta(\tau), \quad (7)$$

where  $e_0$  is the amplitude, for  $e_0 = 1$  gives the equivalent of the zero-temperature bulk coercive field  $e_c$  and  $\theta(\tau)$  is the usual step function.

## RESULTS AND DISCUSSION

Various stages of switching profiles for zero and non-zero  $\delta$  FE films are shown in Fig. 1 and Fig. 2 respectively for temperature  $t = 0.6$ . The starting equilibrium polarization profiles in both cases (Fig. 1 and Fig. 2) are set at negative at time  $\tau = 0$ ; and the profiles are switched by a positive applied electric field  $e$  described in Eq. 7 until it is completely saturated at  $\tau = \tau_s$ .  $\tau_s$  is the switching time, and it is defined as the time taken for the polarization current to decline to 10% of its maximum value [7, 14].

The general trend in polarization reversal of a film, irrespective of value of  $d$ , shows clearly that switching time  $\tau_s$  is longer as the film gets thicker (Fig. 1 and Fig. 2). Fig. 1 (a) and Fig. 1 (b) show the switching profiles of a thinner film ( $l = 3.3$ ) of  $d = 0$  and non-zero  $d$  where all parts of the profiles are shown to switch almost together. There is not much difference in the switching speed between regions near the surface and the interior of the film. In a thicker film ( $l = 7.0$ ), the reversal of polarization begins near the surfaces first, and then goes on to the centre, as shown in Fig 2 (a) and (b). This indicates the domain wall is formed near the surfaces, followed by domain wall movement towards the centre. Hence, when the film becomes thicker, the delay in switching at the centre of the film is more distinct compared with the delay nearer the film surfaces. In term of domain wall movement in the film, it obviously takes a longer time for a domain wall to move from the surface to the

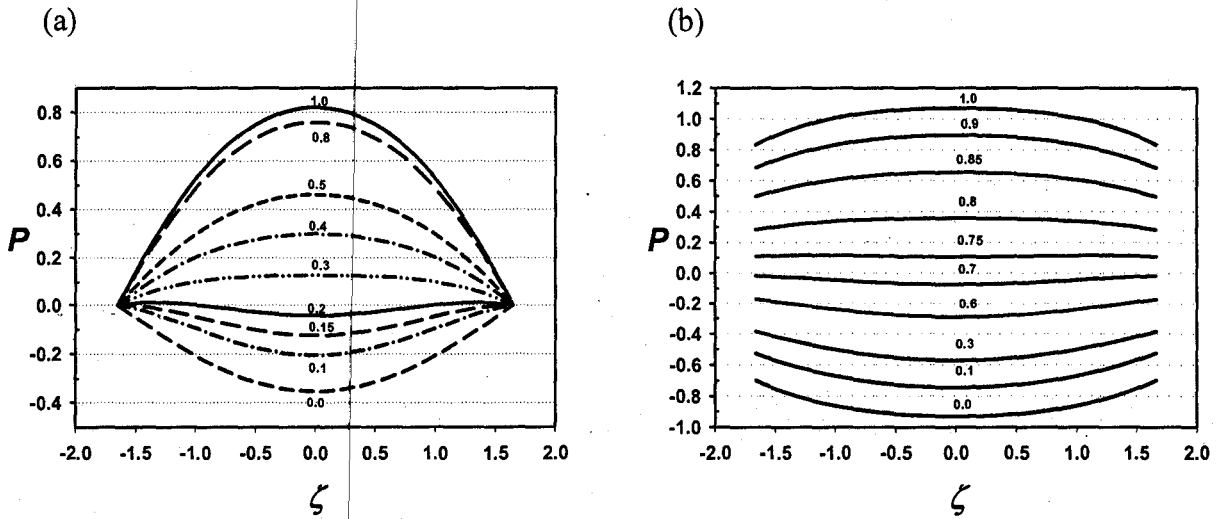


**FIGURE 1** Polarization profiles during switching, at various time in term of fraction of the switching time  $\tau_s$ , at temperature  $t = 0.0$ , applied field  $e = 0.83$ , thickness  $l = 3.3$  for (a)  $\delta = 0$ ; (b)  $\delta = 2.0$ . The number at each curve represents time taken to reach the stage in term of fraction of  $\tau_s$ .

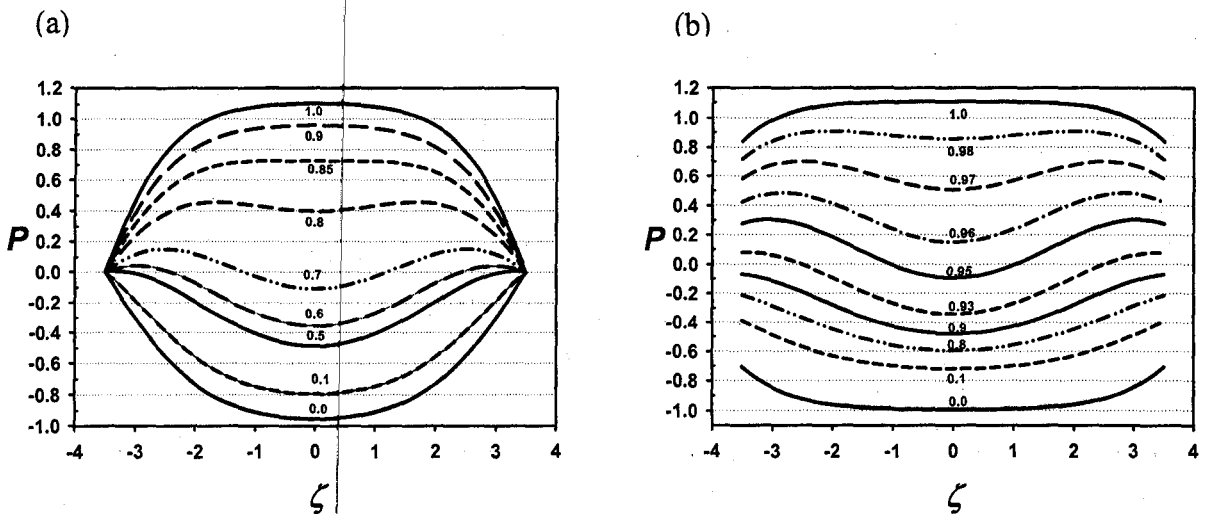


**FIGURE 2.** Polarization profiles during switching, at various time in term of fraction of the switching time  $\tau_s$ , at temperature  $t = 0.0$ , applied field  $e = 0.83$ , thickness  $l = 7.0$  for (a)  $\delta = 0$ ; (b)  $\delta = 2.0$ . The number at each curve represents time taken to reach the stage in term of fraction of  $\tau_s$ .

centre for a thick film than a thin film. It can be seen that the delay in switching at the centre in a zero- $d$  film is more remarkable when the film becomes thicker (Fig. 3).

Fig. 4 shows the average polarization of a FE film versus thickness for various values of  $d$ . It is clear that the extrapolation length  $d$  has great effects on the critical thickness; and the decrease in critical thickness  $l_c$  with increasing value of  $d$  that has been predicted in ref. 11. In addition, the coercive field  $e_{cf}$  of a free boundary film increases with the value of  $d$ . As for a FE film with larger  $d$ , pinning at the surfaces is weak, resulting in a larger surface polarization. Consequently, a larger field is required to reverse the polarization.

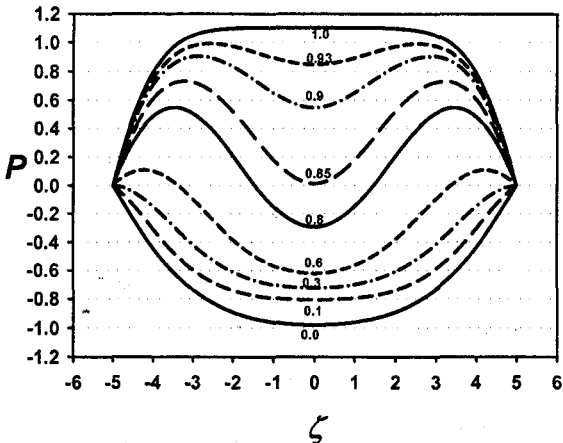


**FIGURE 3** Polarization profiles during switching, at various time in term of fraction of the switching time  $\tau_s$ , at temperature  $t = 0.0$ , applied field  $e = 0.83$ , thickness  $l = 10.0$ ,  $\delta = 0$ .

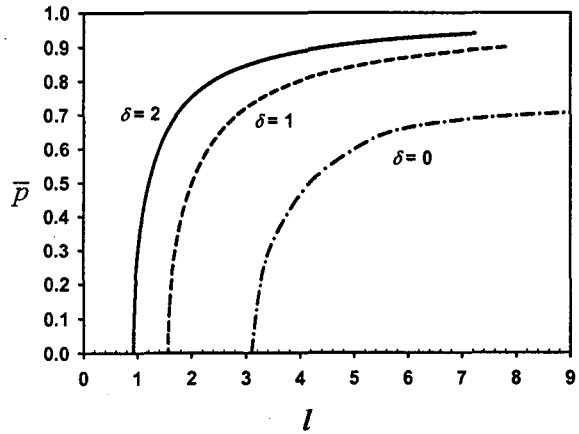


**FIGURE 4** Average polarization versus thickness,  $l$  for various values of  $\delta$ .

## CONCLUSION

The effect of surface conditions, due to  $d$ , on switching behaviours of FE films is studied by using the continuum LD model. It has been shown that switching at the surface and at the centre is almost the same in thin FE films irrespective of  $d$ . For thicker films, surface switching takes place relatively faster than the interior of the films. However, the delay in switching at the centre is more remarkable in the zero- $d$  film as the film thickness increases.

## ACKNOWLEDGEMENTS

The work is funded by the SAGA grant, Academy of Sciences Malaysia (Grant No: 304/PFIZIK/653018/A118).

## REFERENCES

1. W. J. Merz, Phys. Rev. **95**, 690 (1954).
2. E. Fatuzzo and W. J. Merz, in *Ferroelectricity*, 1<sup>st</sup> ed. Edited by E. P. Wohlfarth (Wiley, New York, 1967), Vol. 7, Chap. 7, p: 197.
3. J. F. Scott, *Ferroelectric Memories* (Springer-Verlag, Berlin, 2000)
4. H. Uchida, N. Soyama, K. Kageyama, K. Ogi, and C. A. Paz de Araujo, Integr. Ferroelectr. **8**, 41 (1997)
5. C.S. Ganpule, S. Stanishevsky, Q. Su, S. Aggarwal, J. Mengailis, E. Williams, and R. Ramesh, Appl. Phys. Lett. **75**, 409 (1999)
6. T. Hase and T. Shiosaki, Jpn. J. Appl. Phys. **30**, 2159 (1991).
7. Y. Ishibashi and H. Orihara, J. Phys. Soc. Jpn. **61**, No. 12, 4650-4656 (1992).
8. E. Tokumitsu, N. Tanisaka and H. Ishiwara, Jpn J. Appl. Phys. **33**, 5201-5206 (1994).
9. C. L. Wang and S. R. P. Smith, J. Phys.: Condens. Matter **8**, 4813-4822 (1996).
10. K. H. Chew, J. Osman, R. L. Stamps, D. R. Tilley, F. G. Shin, and H. L. W. Chan, J. Appl. Phys. **93**, 4215 (2003)
11. L. H. Ong, J. Osman, and D. R. Tilley, Phys. Rev. B, **63**, 144109 (2001)
12. P. C. Ooi, Y. Ishibashi, S. C. Lim, and J. Osman, Ferroelrc. **335** (2007)
13. Y. Ishibashi, M. Iwata and A. M. A. Musleh, J. Phys. Soc. Jpn. (2007).
14. T. Katayama, M. Shimizu, and T. Shiosaki, Jpn. J. Appl. Phys. **32**, 3943 (1993)

# Thickness dependence of switching time and coercive field in ferroelectric thin films

Ahmad Musleh, Lye-Hock Ong and Junaidah Osman

Universiti Sains Malaysia, 11800 USM, Penang, Malaysia

E-mail: onglh@usm.my

## Abstract

Switching time and coercive field in polarization reversal of ferroelectric (FE) films have been investigated theoretically by Landau Devonshire free energy expression and Landau Khalatnikov dynamic equation. Our numerical data show that switching time is an exponential function of the applied field and the function implies that there is a definite coercive field in switching for various thicknesses of FE films. In this work, the effects of thickness and surface parameter  $\delta$  on switching time and coercive field have been studied. We found that the coercive field and switching time decrease with decreasing film thickness for film of  $+\delta$ , while the coercive field and switching time increase with decreasing film thickness for film of  $-\delta$ , these results are consistent with the controversial switching phenomena regarding film thickness dependence of coercive field and switching time reported in experiments.

## 1. Introduction

Switching phenomena of FE materials have been actively studied experimentally and theoretically over a long period of time; and the basic understanding of properties of thickness and surface dependence of switching time and coercive field in switching of FE materials is of great importance to the application of FE thin-films in non-volatile memories [1, 2], for example the FE random access memory (FERAM). From the results of earlier work on switching behaviour of single crystal barium titanate ( $\text{BaTiO}_3$ ) [3-7], a few empirical formulations which illustrate the dependence of switching time on applied electric field in switching of FE crystals are cited. For instant, in 1954 Merz [3] reported that switching time  $t_s$  is proportional to  $1/(E - E_c)$  where  $E$  is an applied electric field and  $E_c$  is a kind of coercive field strength. A couple of years later, Merz [4] showed that switching time  $t_s$  versus applied electric field  $E$  for low electric field ( $<10$  kV/cm) for single crystal  $\text{BaTiO}_3$  is an exponential function,  $t_s = t_\infty \exp(\alpha/E)$ , where  $t_\infty$  is the switching time for an infinite field strength and  $\alpha$  is the activation field. This empirical formulation does not imply a definite coercive field in switching of single crystal  $\text{BaTiO}_3$ . A similar empirical formulation for domain wall velocity as an exponential function of applied electric field  $E$  was proposed by Miller and Weinrein [5]; and their formulation also does not imply a definite coercive field in switching of FE crystals. From their formulations, we can deduced that when an electric field  $E$ , however small is applied to a sample, it is just a matter of time; the dipole moments in the sample will ultimately be switched. Around the same period of time, Stadler [6] extended Merz's work on single crystal  $\text{BaTiO}_3$  for high field, ranging from 10 kV/cm to 100 kV/cm; and he found that switching time  $t_s$  is related to applied electric field  $E$  according to a power law:  $t_s = kE^{-n}$ , where  $k$  is a constant and  $n$  is equal to about 1.5. Later, Fatuzzo [7] proposed the combination of the power law and the exponential relation between switching time and applied electric field in his analytical calculations based on the assumption of sideway movement of the domain wall. Again, this new formulation shows that there is no definite coercive field in switching of FE materials. Lately, Klijem and Tadros-Morgane [8] have shown that their experimental data on extrinsic switching time  $\tau_{ex}$  (time taken when the polarization has reached 90% of its maximum value) versus applied electric field  $E$  for various thicknesses of ultra-thin PVDF Langmuir-Blodgett films is not fitted by the formula  $t_s = t_\infty \exp(\alpha/E)$  or by the intrinsic switching formula

$1/t_m = (\frac{E}{E_c} - 1)^{1/2} (1 - \frac{T - T_0}{T_1 - T_0})^{1/2}$  that was derived by Vizdrik *et al.* [9], where  $t_m$  is switching time,  $T_0$  is

the phase transition temperature and  $T_1 = T_0 + 3B^3/4\gamma A$ . This formula indicates the true coercive field for PVDF material and the intrinsic homogeneous switching. They have shown a best fit of their experimental data by a formulation  $\tau_{ex} = \tau_{ex0} \exp(-\eta \frac{E}{E_c})$  with  $\tau_{ex0}$  and  $\eta$  depending on sample thickness, and  $E_c$  is the coercive field of the hysteresis loop.

On the other hand, evidence of a definite coercive field in switching of FE materials has been reported for example in sodium niobate ( $\text{NaNbO}_3$ ) [10, 11]. Another example is from Fousek and Brezina [12, 13], who reported that when the applied voltage on  $\text{BaTiO}_3$  is below a certain threshold value, no domain wall movement has been observed; but when the applied field is above a threshold field, domain wall movement is detected to be out of phase with the applied voltage. Fang and Fatuzzo [14] reported the occurrence of coercive field on bismuth titanate ( $\text{Bi}_4\text{TiO}_{12}$ ). This fact was later proved with measurements on good single crystal by Pulvari (1962, 1964 cited in Fatuzzo and Merz [15] and proved by Cummins [16].

There are a couple of theoretical models proposed to study the switching behaviours of FE films; the Kolmogorov-Avrami-Ishibashi theory [17-19] which is originated from a model of crystal growth [20, 21] and the Landau-typed model [22-25]. In the later model, the numerical data is fitted best by the formula  $t_s = t_\infty \exp(\alpha/E)$  [22], while the authors [24, 25] have fitted their numerical data by the empirical formulations of Merz [3, 4] and Stadler [6] mentioned above; but they have not mentioned which formulation gives the best fit. With these developments in the area of research in switching phenomena of FE materials especially in FE thin films, we are motivated to use Landau Devonshire (L-D) free energy of a FE film proposed by Tilley and Zeks (T-Z) [26] and Landau Khalatnikov equation of motion to look into the dependence of switching time on applied electric field. We have also investigated the effects of thickness on coercive field and switching time and made comparisons with some experimental findings. From the literature, some experimental results [28, 29] show that coercive field increases with decreasing film thickness while others [30, 31] claim the reversed; and these contradictions are explained by the effects of negative and positive values of extrapolation length,  $\delta$  in T-Z model.

## 2. Theory and model.

We consider the T-Z model of L-D free energy for a symmetric FE thin film of thickness  $L$  extending along the  $z$  axis, from  $-L/2$  to  $L/2$  as in the previous papers [26, 27].

$$\frac{F}{S} = \int_{-L/2}^{L/2} \left[ \frac{A(T - T_c)}{2\epsilon_0} P^2 + \frac{B}{4\epsilon_0^2} P^4 + \frac{D}{2\epsilon_0} \left( \frac{dP}{dz} \right)^2 - EP \right] dz + \frac{D}{2\epsilon_0 \delta} (P_-^2 + P_+^2) \quad (1)$$

where  $T_c$  is the bulk transition temperature,  $A$ ,  $B$ , and  $D$  are temperature-independent phenomenological coefficients, in which for second order phase transition  $B$  should be positive. The first two terms inside the integral represent the free energy of FE bulk. The inhomogeneity of the film due to variation of polarization as function of distance  $z$  across the film thickness can be represented by the term  $(dP/dz)^2$ . The surface effect of the film is introduced by including the extrapolation length  $\delta$ . Minimization of the functional (1) leads to the Euler-Lagrange equation

$$D \frac{d^2 P}{dz^2} = A(T - T_c)P + \frac{B}{\epsilon_0} P^3 - E \quad (2)$$

with the following boundary conditions

$$\frac{dP}{dz} = \mp \frac{P}{\delta} \quad \text{at} \quad z = \pm \frac{L}{2} \quad (3)$$

The time variation of polarization during switching can be obtained by the Landau-Khalatnikov (L-K) equation as follows

$$\gamma \frac{\partial P}{\partial \tau} = -\frac{\partial(F/S)}{\partial P} = -\frac{A(T-T_c)}{\epsilon_0} P - \frac{B}{\epsilon_0^2} P^3 + \frac{D}{\epsilon_0} \frac{d^2 P}{dz^2} + E \quad (4)$$

where  $\gamma$  is the viscosity coefficient which causes delay in domain motion. In this equation, the kinetic energy term  $m(\partial^2 P / \partial \tau^2)$  is ignored, since it only contributes to phenomenon in the higher frequency range.

There are several definitions of switching time in the literature [15, 24, 25, 32, 33, 34]. However, we adopt  $\tau_s$  as the switching time where it is the time taken when the current reaches 10% of its maximum value [33, 34]. The reversal of polarization is usually studied experimentally using the step electric field; and the initial polarization in the film is switched from its negative value by the applied field in all the simulations. The dynamic of switching is examined by step driving field of the form

$$E = E_0 \theta(\tau) \quad (5)$$

where  $\theta(\tau)$  is a step function defined as

$$\theta(\tau) \begin{cases} 1 & \text{for } 0 \leq \tau < \tau_0 \\ 0 & \text{for } \tau_0 \end{cases} \quad (6)$$

where  $\tau_0$  is the time when the field is switched off.  $E_0$  is the maximum applied electric field. We obtained the equilibrium polarization profile  $P(z)$  from the elliptic function derived by Ong *et al.* [27], and this profile is symmetric about the film centre  $z = 0.0$ . For the purpose of numerical study, all parameters listed in the equations above are scaled as dimensionless quantities as follows: we put  $t = T/T_c$ ,  $p = P/P_0$  with  $P_0^2 = \epsilon_0 A T_c / B$  and  $e = E/E_c$  with  $E_c^2 = 4A^3 T_c^3 / 27 \epsilon_0 B$ .  $P_0$  and  $E_c$  are the equilibrium bulk polarization and the bulk coercive field at  $T = 0K$  respectively. We let  $\zeta = z/\xi_0$  with  $\xi_0^2 = D/AT_c$  where  $\xi_0$  corresponds to the zero temperature characteristic length of the material and  $l$  is the dimensionless form of  $L$  scaled to  $\xi_0$ , and let  $\delta_r = \delta/\xi_0$ . We define the reduced time  $\tau_r$  by  $\tau_r = \tau(AT_c \xi_0 / \epsilon_0 \gamma)$ . The numerical solutions are obtained by the Runge-Kutta integration with finite difference technique.

### 3. Results and discussion

Figure 1 shows the plot for switching time  $\tau_s$  versus applied field  $e$  for a film of thickness  $l = 2.0$ , extrapolation length  $\delta_r = 3.0$  and temperature  $t = 0.0$ , where all these parameters are in dimensional units. The triangular markers indicated in figure 1 represent the numerical data obtained from our calculations. To investigate whether coercive field truly exists in thin films, curves based on three chosen formulations are drawn to fit the data. The solid-line is drawn based on the formulation by Merz [3] ( $\tau_s = k/(e - \alpha)$ ), where  $e$  is the applied field and  $k$  and  $\alpha$  are constants. From the solid-line curve, we can see that switching time diverges at  $e = \alpha$  where  $\alpha$  is the sort of coercive field; and the FE films can not be switched when  $e < \alpha$ . We have also used the empirical formulation  $\tau_s = \tau_0 \exp(\beta/e)$  [4, 5] where  $\tau_0$  and  $\beta$  are constant, in curve fitting; where the dashed line in figure 1 represents the formulation. Finally we fit our data by the following formulation:

$$\tau_s = \tau_0 \exp[ a/(e - b) ] \quad (6)$$

where  $\tau_0$ ,  $a$  and  $b$  are constants. The switching time  $\tau_s$  diverges when applied electric field  $e$  approaches  $b$ ; and it is shown as dotted-line curve in figure 1. Regression analysis has been carried out in each case of curve fitting (table 1) and based on the regression factors obtained; we find that the simulated data are best fitted by equation (6) with the highest regression factor of 0.99. To ascertain

this fact, a plot of  $\ln \tau_s$  vs.  $1/e$  is shown as the inset (a) of figure 1, where  $\tau_s$  diverges at a certain value which corresponds to  $b$  in the equation which is the presumed coercive field. While inset (b) of figure 1 shows the reciprocal switching time  $1/\tau_s$  versus electric field  $e$ . the reciprocal switching time decreases precipitously towards zero when the field decreases towards the coercive field  $e_{cf}$ . The same trend of  $1/\tau_s$  versus electric field  $e$  for PVDF Langmuir-Blodgett films is shown by Vizdrik *et al.* [9]. Table 1 show the value of the parameters of the above formulation which are used for fitting the data.

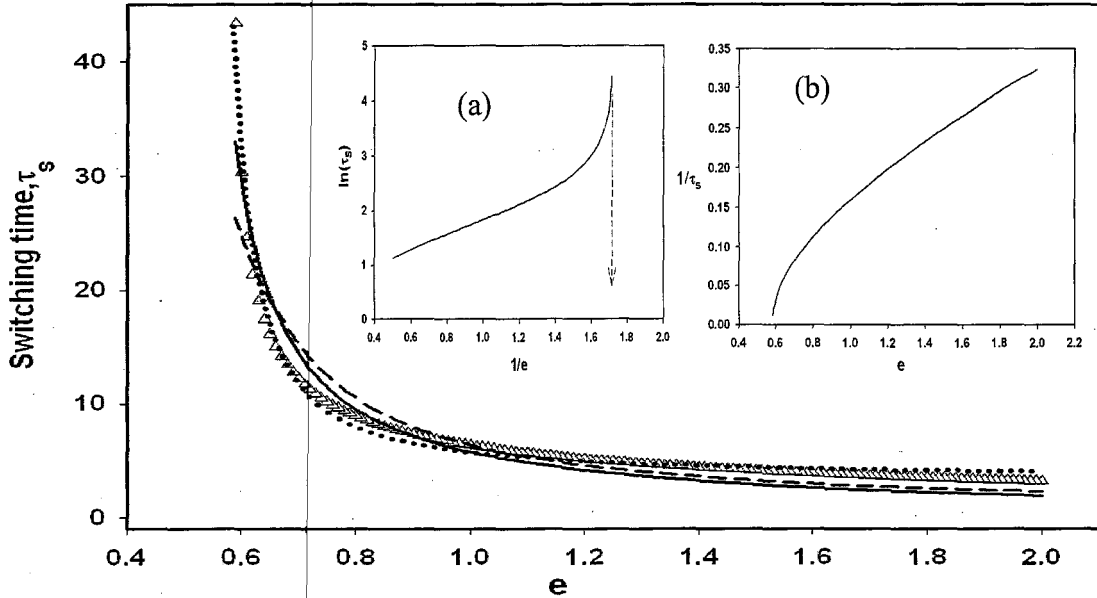


Figure 1 Switching time  $\tau_s$  versus applied electric field  $e$  for dimensionless thickness  $l = 2.0$ , extrapolation length,  $\delta_r = +3$ , and temperature  $t = 0.0$ . Triangle is used to represent the numerical data points. The data are fitted by the following functions: dotted line is for  $\tau_s = \tau_0 \exp[a/(e-b)]$ , solid line is for  $\tau_s = k/(e-\alpha)$ , and dashed line is for  $\tau_s = \tau_0 \exp(\beta/e)$ . The inset (a) shows that  $\ln(\tau_s)$  vs.  $1/e$ , where the dotted arrow indicates the coercive field  $b$  in the function  $\tau_s = \tau_0 \exp[a/(e-b)]$ . The inset (b) shows the reciprocal switching time versus  $e$ .

Table 1 Regression analysis of the numerical data in figure 1.

Formulation	Regression factor	Regression factor square root.	Standard error	The values of the coefficients
$\tau_s = k/(e-\alpha)$	0.9550	0.9119	1.5573	$k = 0.433$ ; $\alpha = 0.579$
$\tau_s = \tau_0 \exp[a/(e-b)]$	0.9891	0.9783	0.7753	$\tau_0 = 6.278$ ; $a = 0.014$ ; $b = 0.577$
$\tau_s = \tau_0 \exp(\beta/e)$	0.9305	0.8658	1.9225	$\tau_0 = 0.793$ ; $\beta = 2.067$

Figure 2 (a), (b) and (c) shows the plot for switching time  $\tau_s$  versus applied field  $e$  for a film of thickness  $l = 2.0$  and negative extrapolation length  $\delta_r = -3.0$  at temperature  $t = 0.0$ . The data (triangle symbol) fitting with the previous formulation emphasize that the electric field dependence of switching time is represented well by equation (6) with high regression factor as shown in table 2. Our calculated data based on the T-Z model for various thicknesses and values of  $\delta_r$ , are fitted by the new formulation in equation (6) with consistent high regression factors; and equation (6) indicates that there is a definite coercive field  $e_{cf}$  with the exponential behaviour.

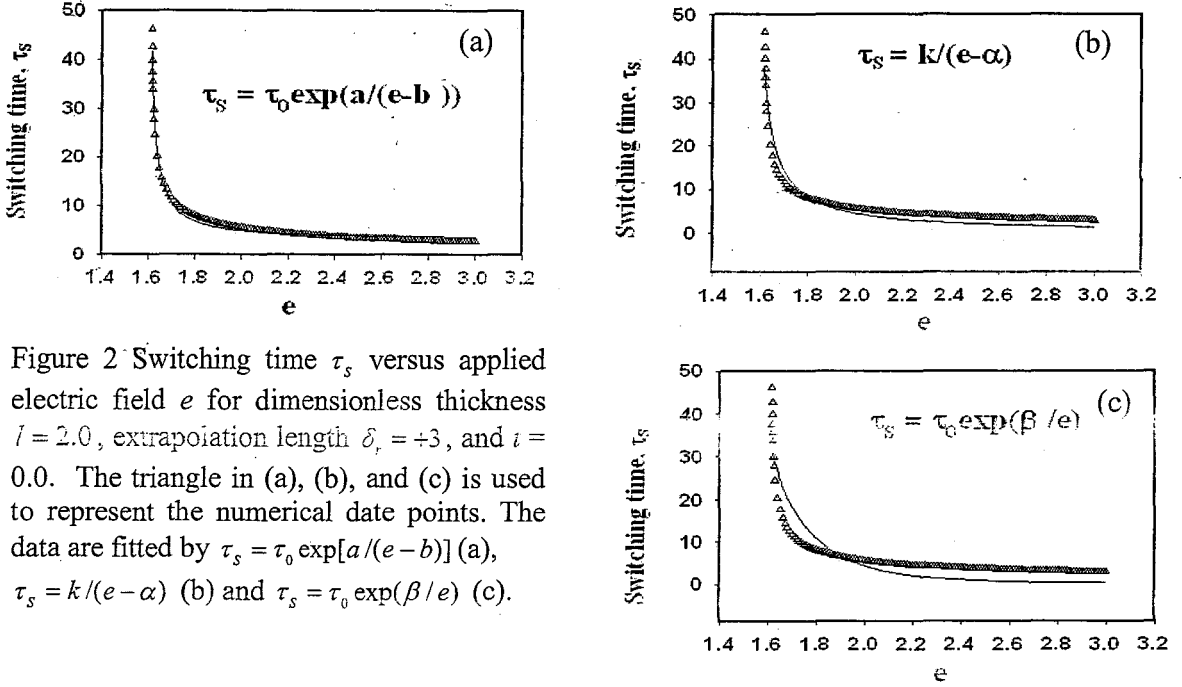


Figure 2 Switching time  $\tau_s$  versus applied electric field  $e$  for dimensionless thickness  $l = 2.0$ , extrapolation length  $\delta_r = +3$ , and  $t = 0.0$ . The triangle in (a), (b), and (c) is used to represent the numerical data points. The data are fitted by  $\tau_s = \tau_0 \exp[a/(e-b)]$  (a),  $\tau_s = k/(e-\alpha)$  (b) and  $\tau_s = \tau_0 \exp(\beta/e)$  (c).

Table 2 Regression analysis of the numerical data in figure 2.

Formulation	Regression factor	Regression factor square root.	Standard error	The values of the coefficients
$\tau_s = k/(e-\alpha)$	0.9711	0.9430	1.9225	$k = 1.9439$ ; $\alpha = 1.5643$
$\tau_s = \tau_0 \exp[a/(e-b)]$	0.9931	0.9863	0.9458	$\tau_0 = 3.3300$ ; $a = 0.1883$ ; $b = 1.5405$
$\tau_s = \tau_0 \exp(\beta/e)$	0.8947	0.8005	3.5973	$\tau_0 = 0.0011$ ; $\beta = 16.5115$

Graphs of  $\tau_s$  versus  $e$  for various film thicknesses  $l$ , and  $+\delta_r$  ( $\delta_r = 3$ ) and  $-\delta_r$  ( $\delta_r = -3$ ) are shown respectively in figure 2 and figure 3. From figure 2 and figure 3,  $\tau_s$  diverges at different values of  $e$  for different thicknesses; and this reveals that the coercive field  $e_{cf}$  is thickness-dependent for both positive and negative  $\delta_r$ .

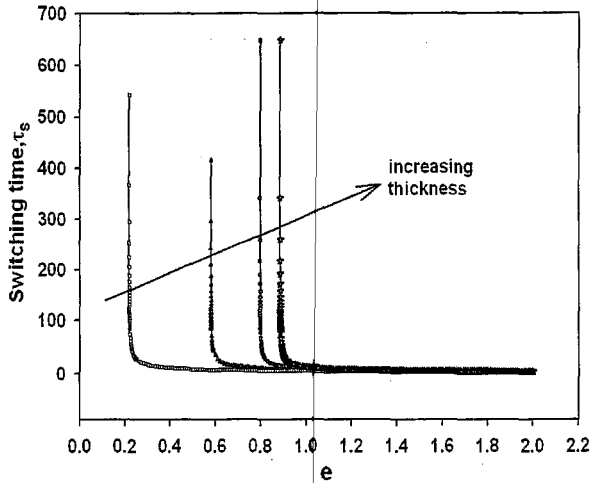


Figure 2 Switching time  $\tau_s$  versus applied electric field  $e$  for various dimensionless thickness,  $l = 1.0, 2.0, 4.0, 6.75$ , temperature  $t = 0.0$ , and extrapolation length  $\delta_r = +3$ . The arrow shows the direction of increasing thickness.

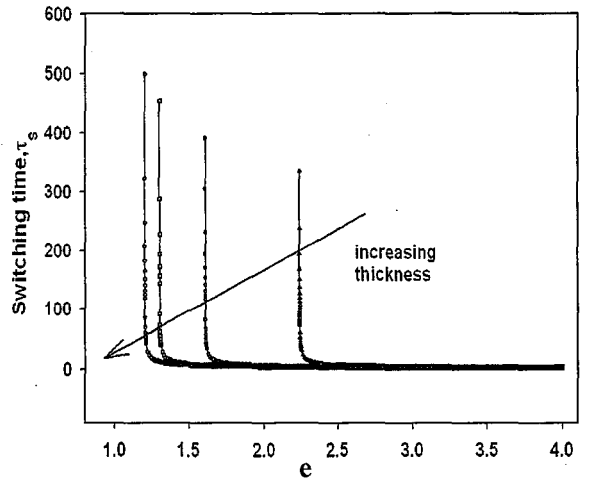


Figure 3 Switching time  $\tau_s$  versus applied electric field  $e$  for various dimensionless thickness,  $l = 1.0, 2.0, 4.0, 5.67$ , temperature  $t = 0.0$ , and extrapolation length,  $\delta_r = -3.0$ . The arrow shows the direction of increasing thickness.

Figure 4 and Figure 5 show the thickness dependence of coercive field for  $+\delta_r$  and  $-\delta_r$ , respectively. In figure 4 we find that for  $+\delta_r$ , the coercive field decreases with decreasing film thickness; and it is consistent with the experimental results [30]. Deduction from equation (2) and equation (3) shows that the initial remnant polarization decreases with decreasing thickness when extrapolation length  $\delta_r$  is positive. This phenomenon is also in agreement with the results obtained from the lattice model [35]. While for negative  $\delta_r$  (figure 5),  $e_{cf}$  increases with decreasing film thickness and these values of  $e_{cf}$  are above  $e_c$  of the bulk. This result is also consistent with experimental results [28, 29].

It is worth giving some comments on figure 4 and figure 5, for  $+\delta_r$  (figure 4), it is interesting to see that the coercive field has finite size behaviour similar to that of the Curie temperature [36-38]. FE phase vanishes at certain critical thickness, in which the material exhibits size-driven phase transition [39]. Extrapolating the three curves to meet the horizontal axis in figure 4 gives the critical thickness of 0.68, 0.24 and 0.04 for  $\delta_r = 3.0, 10.0$  and 50.0 respectively. While for  $-\delta_r$  (figure 5), it is clear that there is no size-driven phase transition.

The effects of surface (influenced by  $\delta_r$ ) on the coercive field of the film  $e_{cf}$  can be seen from figure 4 for  $+\delta_r$  and from figure 5 for  $-\delta_r$ . For a film of given thickness, increasing value of  $+\delta_r$ , increases the coercive field of the film. From figure 4, it is obvious that for a film of large value of  $+\delta_r$  and large thickness value  $l$  (thicker film), the coercive field approaches the value  $e_c = 1$ , where  $e_c$  is the dimensionless coercive field of the bulk, at temperature  $t = 0.0$ . In contrary to a film with surface effect of  $+\delta_r$ , it is clearly shown in figure 5 that in a thin film of small thickness value  $l$  with surface effect of  $-\delta_r$ , the coercive field of the film increases with increasing surface effect, (that is for smaller magnitude of  $|\delta_r|$ ). However, surface effect becomes weaker as the film becomes thicker as illustrated in figure 5 where the coercive fields of thick films with different magnitudes of  $-\delta_r$

approach the bulk coercive field; so  $e_{cf}$  is small even for smaller  $|\delta_r|$ . It is interesting to see that surface effect which is parameterized by the extrapolation length  $\pm\delta_r$  in this model is more significant for thin films (small values of thickness  $l$ ); but for thick films, surface effect is weak and it is almost negligible.

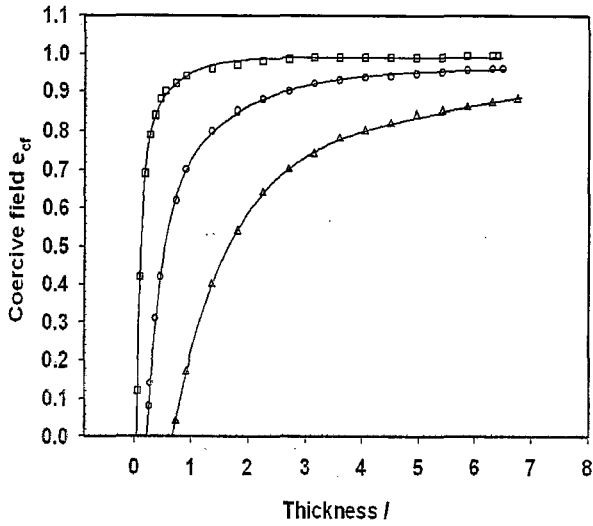


Figure 4 Coercive field  $e_{cf}$  versus film thickness  $l$  for various positive extrapolation length  $\delta_r$ , and temperature  $t = 0.0$ . Symbols: Triangle for  $\delta_r = +3$ , circle for  $\delta_r = +10$  and square for  $\delta_r = +50$ .

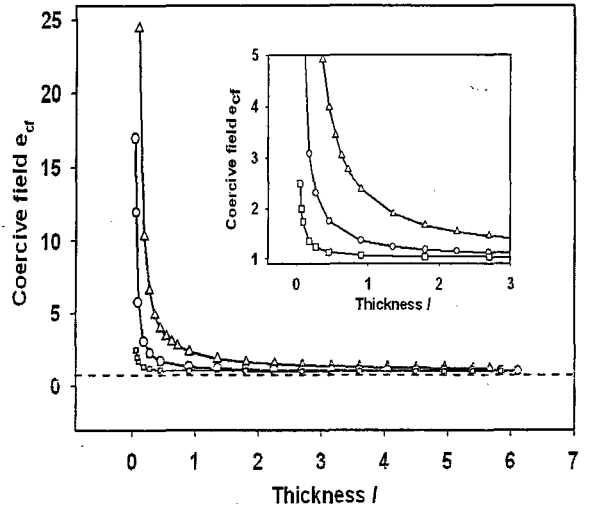


Figure 5 Coercive field  $e_{cf}$  versus film thickness  $l$  for various negative extrapolation length  $\delta_r$ , and temperature  $t = 0.0$ . Symbols: Triangle for  $\delta_r = -3$ , circle for  $\delta_r = -10$  and square for  $\delta_r = -50$ . The dashed line is bulk coercive field value  $e_c = 1.0$ . The inset shows the zoom in view for a range of  $l \leq 3$ .

In general, switching time is affected by the film thickness. For  $+\delta_r$ , the effect of thickness on switching time is shown in figure 6. For a given applied electric field  $e$ , switching time  $\tau_s$  is shorter for thinner film, and it is consistent with the experimental results of Mitoseriu *et al.* [40]. From figure 6, it reveals that the thickness dependence switching time  $\tau_s$  is qualitatively similar to the variation of coercive field  $e_{cf}$  with film thickness (figure 4). Figure 6 shows that for a film of a given thickness and with small value of  $+\delta_r$  has shorter switching time; and the effect of surface effect ( $+\delta_r$ ) on switching time is more significant for thin films. For  $-\delta_r$ , the effect of thickness on switching time shown in figure 7, at a given applied field  $e$ , it can be seen that by decreasing the film thickness, switching time increases and this result is consistent with the recent experimental measurement [8]. Figure 7 shows that there is no size-driven phase transition for films with  $-\delta_r$ . While for a film of a given thickness with  $-\delta_r$ , switching time becomes longer for smaller magnitudes of  $|\delta_r|$ ; and here again surface effect is more profound for thin films. These results which are shown to be related to the surface parameter  $-\delta_r$  can be explained based on equation (2) and equation (3) that decreasing  $|\delta_r|$  for a given thickness, increases the initial remnant polarization, switching of the dipole moments would taken a longer time.

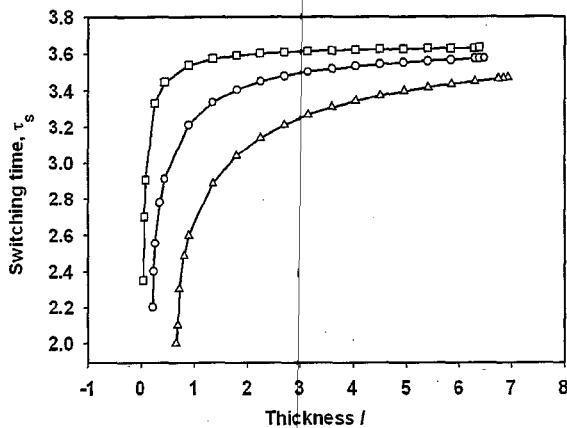


Figure 6 Switching time  $\tau_s$  versus film thickness  $l$  for various positive extrapolation length  $\delta_r$ , applied electric field  $e = 2.0$ , and temperature  $t = 0.0$ . Symbols: Triangle for  $\delta_r = 3.0$ , circle for  $\delta_r = 10.0$  and square for  $\delta_r = 50.0$ .

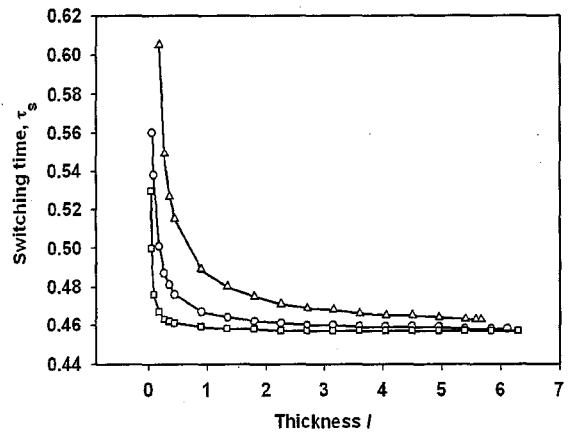


Figure 7 Switching time  $\tau_s$  versus film thickness  $l$  for various negative extrapolation length  $\delta_r$ , applied electric field  $e = 25.0$  (We used high field here in order to switch the ultra thin film of small  $|\delta_r|$ ), and temperature  $t = 0.0$ . Symbols: Triangle for  $\delta_r = -3.0$ , circle for  $\delta_r = -10.0$  and square for  $\delta_r = -50.0$ .

#### 4 Summary

Landau-typed T-Z model is used to study the intrinsic switching phenomena of a free standing film. A new function is proposed for switching time dependence of electric field reveals the true intrinsic coercive field  $e_{cf}$  of a FE film. It is found that  $e_{cf}$  increases with increasing film thickness for positive extrapolation length  $\delta_r$ ; and decreases with increasing film thickness for negative extrapolation length  $\delta_r$ . While, switching time  $\tau_s$  of a FE film increases with increasing film thickness for  $+\delta_r$ ; and decreases with film thickness for  $-\delta_r$ . The surface effect ( $\pm\delta_r$ ) on switching time and coercive field of a FE film is more spectacular especially for thinner films.

#### Acknowledgment

The work is funded by the SAGA grant, Academy of Sciences Malaysia (Grant No: 304/PFIZIK/653018/A118). We sincerely acknowledge Prof. David R. Tilley for giving his invaluable views.

#### References

- [1] Scott J F 2000 *Ferroelectric Memories* (Germany: Springer-Verlag)
- [2] Dawber M, Rabe K M and Scott J F 2005 *Rev. Modern physics* **77** 1083
- [3] Merz W J 1954 *Phys Rev.* **95** 690
- [4] Merz W J 1956 *Appl. Phys.* **27** 938
- [5] Miller R C and Savage A 1958 *Phys. Rev.* **112** 755.
- [6] Stadler H L 1958 *J. Appl. Phys.* **29** 1485
- [7] Fatuzzo E 1962 *Phys. Rev.* **127** 1999
- [8] Kliem H and Tadros-Morgane R 2005 *J. Phys. D: Appl. Phys.* **38** 1860
- [9] Vizdrik G, Ducharme S, Fridkin V M and Yudin S G 2003 *Phys. Rev. B.* **68** 094113
- [10] Pulvari C F 1960 *Phys. Rev.* **120** 1670
- [11] Miller R C, Wood E A, Remeika J P and Savage A 1962 *J. Appl. Phys.* **33** 1623.
- [12] Fousek J and Brezina B 1960 *Czech. J. Phys.* **B10** 511 and 1961 **B11** 344.

- [13] Fousek J and Brezina B 1964 *J. Phys. Soc. Jpn.* **19** 830
- [14] Fang P H and Fatuzzo E 1962 *J. Phys. Soc. Jpn* 17 238
- [15] Fatuzzo E and Merz W J 1967 *Ferroelectricity* (Amsterdam: North-Holland)
- [16] Cummins S E 1965 *J. Appl. Phys.* **36** 1958
- [17] Ishibashi Y and Orihara H 1992 *J. Phys. Soc. Jpn.* **61** 650
- [18] Orihara H and Ishibashi Y 1992 *J. Phys. Soc. Jpn.* **61** 1919
- [19] Ishibashi Y 1993 *Integrated Ferroelectr.* **3** 351
- [20] Kolmogorov A K 1937 *Izv. Akad. Nauk. Math.* **3** 355
- [21] Avrami M 1939 *J. Chem. Phys.* **7** 1103; 1940 *J. Chem. Phys.* **8** 212; 1941 *J. Chem. Phys.* **9** 177
- [22] Ishibashi Y 1992 *Jpn. J. Appl. Phys.* **31** 2822
- [23] Wang C L and Smith S R P 1996 *J. Phys.: Condens. Matter* **8** 4813
- [24] Ishibashi Y 1990 *J. Phys. Soc. Jpn.* **59** 4148
- [25] Nagaya T and Ishibashi Y 1991 *J. Phys. Soc. Jpn.* **60** 4331
- [26] Tilley D R and Zeks B 1984 *Solid State Commun.* **49** 823
- [27] Ong L-H, Osman J and Tilley D R 2001 *Phys.Rev. B* **63** 144109
- [28] Hase T and Shiosaki T 1991 *Jpn J. Appl. Phys.* **30** 2159
- [29] Fujisawa H, Nakashima S, Kaibara K, Shimizu M, and Niu H 1999 *Jpn. J. Appl. Phys. Part 1* **38** 5392
- [30] Wang M C, Hsiao F Y, His C S and Wu N C 2002 *J. of Crystal Growth.* **246** 78
- [31] Yanase N, Abe K, Fukushima N and Kawakuko T 1999 *Jpn. J. Appl. Phys.* **38** 5305
- [32] Ishibashi Y 1992 *Jpn. J. Appl. Phys.* **31** 2822
- [33] Omura M, Adachi H, and Ishibashi Y 1992 *Jpn. J. Appl. Phys.* **31** 3238.
- [34] Katayama T, Shimizu M and Shiosaki T 1993 *Jpn. J. Appl. Phys.* **32** 3943
- [35] Ricinschi D, Harangea C, Papusoi C, Mitoseriu L, Tura V and Okuyama M 1998 *J. Phys.: Condens. Matter* **10** 477
- [36] Zhong W L 1994 *Physica Letters A* **189** 121
- [37] Wang Y G, Zhong W L and Zhang P L 1994 *Solid State Commun.* **92** No. 6 519
- [38] Wang C L and Smith S R P 1995 *J. Phys.: Condens. Matter* **7** 7163
- [39] Ishibashi Y, Orihara H and Tilley D R 1998 *J. Phys. Soc. Jpn.* **67** 3292
- [40] Mitoseriu L, Ricinchi D, Harnagea C and Okuyama M 1996 *Jpn. J. Appl. Phys.* **35** 5210

## Tilley-Zeks Model in Switching Phenomena of Ferroelectric Films

Lye-Hock Ong\*, Ahmad Musleh

School of Physics, Universiti Sains Malaysia,  
11800 USM, Penang, Malaysia.

\*Corresponding author, E-mail address: [onglh@usm.my](mailto:onglh@usm.my)

**Keywords** Landau theory; polarization reversal; surface effect; size effect

**PACS numbers:** 77.80.Fm; 78.20Bh

### Abstract

We use the Tilley-Zeks model of Landau Devonshire free energy and the Landau Khalatnikov equation of motion to elucidate the phenomena of polarization reversal of second-order ferroelectric films, particularly the characteristics of hysteresis loops by the applied field and the response of bipolar pulses by the films. It is shown that at constant temperature, the size of hysteresis loops increases with increasing film thickness for  $+\delta$  and the reverse is true for  $-\delta$ . For a film of fixed thickness, the size of hysteresis loop decreases with increasing temperature for both cases of  $+\delta$  and  $-\delta$ . The model has also demonstrated the effects of magnitude and frequency of the applied field on the hysteresis loops are similar to the experimental results.

### 1. Introduction

The trend of device fabrication to have higher packing density per unit area has led to the reduction in size of individual components. In particular, miniaturization of the components has aggravated surface and size effects that influence the properties of ferroelectric (FE) thin films and nano-sized particles [1-2], such as dielectric properties, critical temperature, spontaneous polarization and etc. There are a small number of models formulated to elucidate on switching properties of FE thin films; the Kolmogorov-Avrami-Ishibashi (KAI) theory based on the crystal growth theory [3], discrete model based on the

Landau-type-free energy [4, 5], and the non-KAI model proposed by Tagantsev *et al* [6]. Tilley-Zeks (T-Z) model of Landau Devonshire (LD) free energy expression has been successfully used to study the phase transition and dielectric properties of FE thin films [7-12]. The significant of the model is the inclusion of parameter  $\delta$ , the extrapolation length in the free energy for the surface effect, which was proposed by Krestchmer and Binder [13] that polarization at the surfaces can either be suppressed, by setting  $\delta$  to be positive, or surface polarization can be enhanced when  $\delta$  is set as negative. Hence,  $\delta$  affects the spontaneous polarization at the surfaces of a film, and on the whole, the average polarization of the film. The suppression or enhancement of surface polarization compared to the polarization inside the film has a considerable influence on switching behaviours of FE films.

## 2. Theory and Modeling

The free energy model in dimensionless units is for a one-dimensional FE thin film, with polarization and related physical quantities varying as a function of distance  $\zeta$ , and the direction of polarization can be parallel to the film surfaces or perpendicular to the film surfaces for perovskite FE materials which are set in contact with electrodes; so the depolarization effects can be neglected [14]. It is a symmetric film of thickness  $l$  extending along the  $\zeta$  axis, from  $-l/2$  to  $l/2$ ; and the FE material is assumed to undergo a second-order phase transition. The scaling on units involved in the subsequent discussion is the same as that given in ref. 8 and 15; and due to the constraint of space, the discussion will not be repeated here. Hence, the dimensionless form of Landau-Devonshire (L-D) free energy  $f$  per unit surface area for a thin film with thickness  $l$  under an action of an external electric field  $e$  is expressed as

$$f = \int_{-l/2}^{l/2} \left[ \frac{t-1}{2} p^2 + \frac{1}{4} p^4 + \frac{1}{2} \left( \frac{dp}{d\zeta} \right)^2 - \frac{2}{3\sqrt{3}} ep \right] d\zeta + \frac{1}{2\delta_r} (p_-^2 + p_+^2) \quad (1)$$

The inhomogeneity of the film due to variation of polarization as function of distance  $\zeta$  across the film thickness can be represented by the term  $(dp/d\zeta)^2$ . As mentioned earlier,  $\delta_r$  is a reduced parameter of  $\delta$  which relates to the surface effect of the film. Minimization of the functional leads to the Euler-Lagrange equation

$$\frac{d^2 p}{d\zeta^2} = \frac{(t-1)}{2} p + p^3 - \frac{2}{3\sqrt{3}} e \quad (2)$$

with the following boundary conditions

$$\frac{dp}{d\zeta} = \mp \frac{p}{\delta_r} \quad \text{at } \zeta = \pm \frac{l}{2} \quad (3)$$

The scaled Landau Khalatnikov (LK) equation is as follows

$$\frac{\partial p}{\partial \tau_r} = -\frac{\partial f}{\partial p} = (1-t)p - p^3 + \frac{d^2 p}{d\zeta^2} + \frac{2}{3\sqrt{3}} e \quad (4)$$

The global order parameter is the average polarization of the film defined as

$$\bar{p} = \frac{1}{l} \int_{-l/2}^{l/2} p(\zeta) d\zeta. \quad (5)$$

### 3. Numerical Method

The initial polarization profile of the FE film at  $e = 0.0$  is obtained from eq. 2 by using the elliptic function derived in ref. 8. In all our simulations, the initial polarization in the film is switched from its negative value. By solving eq. 4 using the Runge-Kutta integration by finite difference technique, we obtained the reversal of polarization. The reversal of polarization is studied by an applying sinusoidal field that is usually used in experiments. The sinusoidal field in the reduced form is

$$e = e_0 \sin(\omega\tau_r), \quad (6)$$

where  $e_0$  is the amplitude and  $\omega$  is the angular frequency.

#### 4. Results and discussion

The influence of the sinusoidal electric field strength  $e_0$  on the FE hysteresis loop for a given temperature  $t = 0.0$ , thickness  $l = 5.0$  (thick film), frequency  $\omega = 0.08$  and positive extrapolation length  $\delta_r = +3.0$  is shown in Fig. 1. From the figure, it is clear that the FE characteristics are strongly dependent on electric field strength  $e_0$ . The average remnant polarization  $\bar{p}_r$  does not increase remarkably in a thick film; and its polarization is closed to the bulk value. However, for thin film the average remnant polarization  $\bar{p}_r$  increases with increasing  $e_0$  (Fig. 2). This result is consistent with the experimental result [16] and the theoretical result given by Omura *et al.* [17] using the lattice model.

Figure 3 shows the hysteresis loops for various frequencies  $\omega$  for a FE film of thickness  $l = 1.35$ ,  $t = 0.0$ ,  $\delta_r = +3$  and  $e_0 = 2.5$ . Increasing  $\omega$  leads to increase in coercive field  $e_{cf}$  and average remnant polarization  $\bar{p}_r$ . Physically, the reason for the increase of  $e_{cf}$  with  $\omega$  is that at higher frequency the speed of domain movement increases and hence the material is made more 'viscous'; thus the system needs more energy when it is switched from one state to another. This result is consistent with experimental results by Lohse *et al.* [18] and Picinin *et al.* [19] regarding the increase in values of  $e_{cf}$  with at higher values of  $\omega$ . But in Picinin *et al.*'s report,  $\bar{p}_r$  decreases with increasing  $\omega$ ; and it may be attributed to the defects (oxygen vacancies) present in  $\text{Pb}(\text{Zr}_{0.53}, \text{Ti}_{0.47})\text{O}_3$  (PZTN) doped with  $\text{Nb}_2\text{O}_5$  donor which causes the domain wall pinning that reduces the number of switchable dipoles. Similar features of increasing coercive field  $e_{cf}$  and average remnant polarization  $\bar{p}_r$  with increasing  $\omega$  are obtained for FE film with  $-\delta_r$ ; so the discussion of the results will not be repeated here.

The effect of the temperature  $t$  on the hysteresis loop for positive and negative  $\delta_r$ 's can be observed from the curves in Fig. 4 and Fig. 5. It can be seen that the system at higher temperature needs lower applied electric field  $e$  to switch; and the average polarization  $\bar{p}_r$  is lower at higher temperature as the system is at a state which is nearer to the phase transition. These results are consistent with experimental results given by Yuan *et al.* [20]; and from their studies on strontium Bismuth Titanate  $\text{Sr}_2\text{BiTi}_3\text{O}_{12}$  (SBT) which has lower density of oxygen vacancies, so the pinning of domain wall is weak. However our result is not consistent with the experimental results given by Zhang *et al.* [21] on  $\bar{p}_r$  where they used  $\text{Ba}_{3.25}\text{La}_{0.75}\text{Ti}_3\text{O}_{12}$  (BLT) that has high density of oxygen vacancies which tends to be trapped at the domain boundaries. The oxygen vacancies formed the domain walls pinning centres and hence reduce the number of switchable dipoles. Nevertheless, our study is consistent with the theoretical results of lattice model reported by Tura *et al.* [5]. Similar features of decreasing size of hysteresis loops with increasing temperature for both positive and negative signs of  $\delta_r$  given in their results are found in Fig. 4 and Fig. 5.

The effects of thickness  $l$  on hysteresis loops are illustrated in Fig. 6 and Fig. 7 for  $+\delta_r$  and  $-\delta_r$  respectively. Fig. 6 reveals that for a given  $+\delta_r$ ,  $e_{cf}$  and  $\bar{p}_r$  increases with increasing thickness and it is consistent with the experimental results by Wang *et al.* and Yanase *et al.* [22, 23]. These results are also in agreement with the results obtained from the lattice model [24]. On the contrary, Hase *et al.* and Fujusawa *et al.* in their hysteresis loops measurements [25, 26] found that  $e_{cf}$  decreases with increasing film thickness; and this trend of thickness dependence of  $e_{cf}$  is found in Fig. 7. In Fig. 7, it reveals that for  $-\delta_r$ , both  $e_{cf}$  and  $\bar{p}_r$  decrease with increasing thickness and these values of  $e_{cf}$  are above  $e_{cB}$  of the bulk.

However,  $\bar{p}_r$  is reported to increase with increasing thickness by Hase *et al.* [25]; but Fujusawa *et al.* [26] reported that  $\bar{p}_r$  is almost unchanged with thickness.

Surface effects of FE films are represented via the effects of positive and negative extrapolation lengths on hysteresis loop are shown in Fig. 8 and Fig. 9 for  $+\delta_r$  and  $-\delta_r$  respectively. Both values of  $e_{cf}$  and  $\bar{p}_r$  increase with increasing values of  $+\delta_r$  (Fig. 8). This effect can be explained by the increase of initial polarization profile with increasing values of  $+\delta_r$ . It is obvious from Fig. 9 that increasing  $|\delta_r|$ , which leads to decreasing surface polarization, tends to decrease  $e_{cf}$  and  $\bar{p}_r$ .

Figure 10 shows the response of average polarization  $\bar{p}$  and switching current generated by applying bipolar pulses (the inset of Fig. 10). The pulse width  $\tau_w$  is controlled so that it is larger than the switching time  $\tau_s$ . The full switching current and the non-switching current are generated by the pulses  $p_1$  and  $p_2$  respectively for forward switching and by the pulses  $p_3$  and  $p_4$  for back forward switching respectively. The intrinsic switching current can be evaluated by subtracting non-switching transient current from the full switching transient current. Back switching phenomenon is indicated by vertical arrows. During the back switching, when the applied field is removed, the system relaxes to the equilibrium remnant average polarization. The degree of back switching measures the magnitude of field induced polarization. Experimentally, Chae *et al.* [27] reported the similar polarization response by the applied bipolar pulses as we have shown in this work.

## 5. Conclusion

The results we obtained from the T-Z model on the response of dynamic electric field on FE thin films discussed in the previous section go along well with the experimental

observations and the numerical results given by the discrete model. As a summary, Table 1 is included to show the comparisons between the calculated results and experimental outcomes. The extrapolation length  $\delta_r$ , incorporated in the free energy, is the significant of T-Z model in comparison with the other models; and from our calculations the parameter which relates to the surface ordering has shown to have considerable effects on switching phenomenon of FE materials. Contrary trends on thickness dependence of coercive field of FE films in experimental results can be explained by the effects of  $+\delta_r$  and  $-\delta_r$ . Surface effects on switching of FE films are revealed via the effects of  $+\delta_r$  and  $-\delta_r$  on the characteristics of hysteresis loops which show that  $e_{cf}$  and  $\bar{p}_r$  increase with the increasing magnitude of  $+\delta_r$ ; and the reverse is true for FE films with the characteristic of  $-\delta_r$ .

### Acknowledgement

The work is funded by the SAGA grant, Academy of Sciences Malaysia (Grant No: 304/PFIZIK/653018/A118). We thank Prof. David R. Tilley & Dr. Junaidah Osman for their helpful discussion.

### References

1. Moazzami R.; *Semicond. Sci. Technol.* **10**, p375 – 390 (1995).
2. Scott J. F.; *Ferroelectrics memories*. (Berlin, Springer, 2000).
3. H. Orihara, S. Hashimoto, and Y. Ishibashi, *J. Phys. Soc. Jpn.* **63**, 1031 (1994).
4. Y. Ishibashi, *J. Phys. Soc. Jpn.* **59**, 4148 (1990).
5. Tura V., Ricinschi D., Mitoseriu L., Harnagea C., Ando S., Tsukamoto T., and Okuyama M.; *Jpn. J. Appl. Phys.* **36**, 2183 (1997).
6. A. K. Tagantsev, I. Stolichnov, N. Setter, J. S. Cross, and M. Tsukada, *Phys. Rev. B* **66**, 214109 (2002).
7. Tilley D.R. and Zeks B.; *Solid State Commun.* **49**, 823-827 (1984).
8. Ong L. H., Osman J. and Tilley D. R.; *Physical Review B* **63** (14), 144109 (2001).
9. Zhong W. L., Qu B. D., Zhang P. L. and Wang Y. G.; *Phys. Rev. B* **50**, 12375-12380 (1994).

10. Scott J. F., Duiker H. M., Beale P. D., Pouligny B., Dimmler K., Parris M., Butler D., and Eaton S.; *Physica B* **150**, 160-167 (1988).
11. Ishibashi Y., Orihara H. and Tilley D. R.; *J. Phys. Soc. Jpn.* **67**, 3292-3297 (1998).
12. Tan E. K., Osman J., and Tilley D.R.; *Solid State Commun.* **116**, 61-65 (2000).
13. Kretschmer R. and Binder K.; *Phys. Rev. B* **20** (3) 1065 (1979).
14. Watanabe Y.; *Phys. Rev. B*, **57**, 789 (1998).
15. Ahmad M., Ong L. H., and Osman J.; submitted to *J. Appl. Phys.* (2008).
16. Tokumitsu E., Tanisake N., and Ishiwara H.; *Jpn. J. Appl. Phys.* **33**, 5201 (1994).
17. Omura M., Adachi H., and Ishibashi Y.; *Jpn. J. Appl. Phys.* **30**, 2384 (1991).
18. Lohse O., Grossmann M., Boettger U., Bolten D., and Waser R.; *J. Appl. Phys.* **89**, 2332 (2001).
19. Picinin A., Lente M. H., Eiras J. A., and Rino J P.; *Phys. Rev. B* **69** 064117 (2004).
20. Yuan G. L., Liu J. M., Baba-Kishi K., Chan H. L. W., Choy C. L. and Wu D.; *Materials Science and Engineering B* **118**, 225 (2005).
21. Zhang S.-T., Yuan G.-L., Wang J., Chen Y.-F., Cheng G.-X., and Liu Z.-G.; *Solid State Commun.* **132**, 315 (2004).
22. Wang M. C., Hsiao F.-Y., Hsi C.-S., and Wu N.-C.; *J. Crystal Growth* **246**, 78 (2002).
23. Yanase N., Abe K., Fukushima N., and Kawakubo T.; *Jpn. J. Appl. Phys.* **38**, 5305 (1999).
24. Ricinschi D., Harnagea C., Papusoi C., Mitoseriu L., Tura V., and Okuyama M.; *J. Phys.: Condens. Matter* **10**, 477 (1998).
25. Hase T., and Shiosaki T.; *Jpn. J. Appl. Phys.* **30**, 2159 (1991).
26. Fujisawa H, Nakashima S, Kaibara K, Shimizu M and Niu H; *Jpn. J. Appl. Phys.* **38**, 5392-6 (1999).
27. Chae B. G., Lee J. S., Yang Y. S., Kim S. H., and Jang M. S.; *Jpn. J. Appl. Phys.* **36**, 7275 (1997)

## Figure and Table Captions

- Figure 1. Hysteresis loops for various values of field strength  $e_0$ : 0.91, 1.0, 1.5, 2.0; and  $l = 5.0, t = 0.0, \delta_r = +3, \omega = 0.08$ .
- Figure 2. Hysteresis loops for various values of field strength  $e_0$ : 0.6, 1.0, 2.0; and  $l = 1.35, t = 0.0, \delta_r = +3, \omega = 0.09$ .
- Figure 3. Hysteresis loops for various values of frequency  $\omega$ : 0.03, .09, 0.2, 0.3; and  $l = 1.35, t = 0.0, \delta_r = +3, e_0 = 2.5$ .
- Figure 4. Hysteresis loops for various values of temperature  $t$ : 0.0, 0.2, 0.6.; and  $l = 2.00, e_0 = 3.0, \omega = 0.1, \delta_r = +3.0$ .
- Figure 5. Hysteresis loops for various values of temperature  $t$ : 0.0, 0.2, 0.6; and  $l = 2.00, e_0 = 3.0, \omega = 0.1, \delta_r = -3.0$ .
- Figure 6. Hysteresis loops for various values of film thickness  $l = 0.72, 2.0, 5.0$ ; and  $e_0 = 3.0, \delta_r = 10.0, \omega = 0.1, t = 0.0$ .
- Figure 7. Hysteresis loops for various values of film thickness  $l = 0.72, 2.0, 5.0$ ; and  $e_0 = 3.0, \delta_r = -10.0, \omega = 0.1, t = 0.0$ .
- Figure 8. Hysteresis loops for various values of positive extrapolation length  $\delta_r = 3.0, 10.0, 50.0$ ; and  $l = 0.72, t = 0.0, e_0 = 3.0, \omega = 0.1$ .
- Figure 9. Hysteresis loops for various values of negative extrapolation length  $\delta_r = -3.0, -10.0, -50.0$ ; and  $l = 0.72, t = 0.0, e_0 = 3.0, \omega = 0.1$ .
- Figure 10. Average Polarization (dashed curve) and current (solid line) versus time, using bipolar-pulse field.  $l = 1.8, \delta_r = +3, e = 1.0, t = 0.0$ .  $\tau_s$  is the switching time and  $\tau_w$  is the pulse width.
- Table 1. Comparison of Calculated results with experimental results.

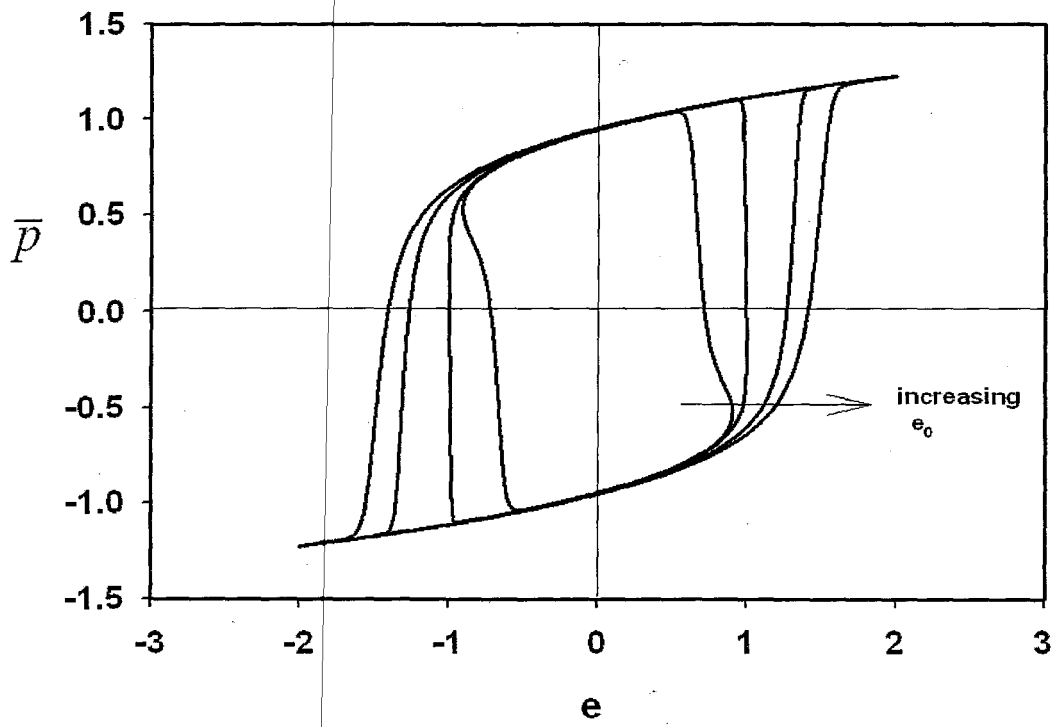


Fig. 1

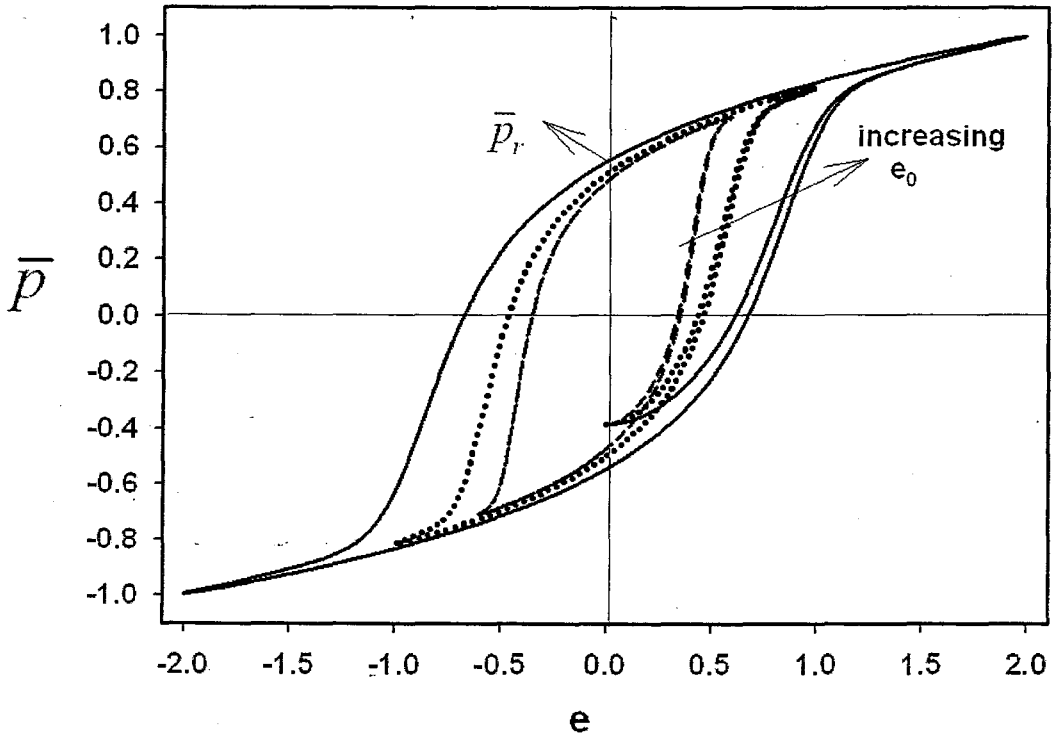


Fig. 2

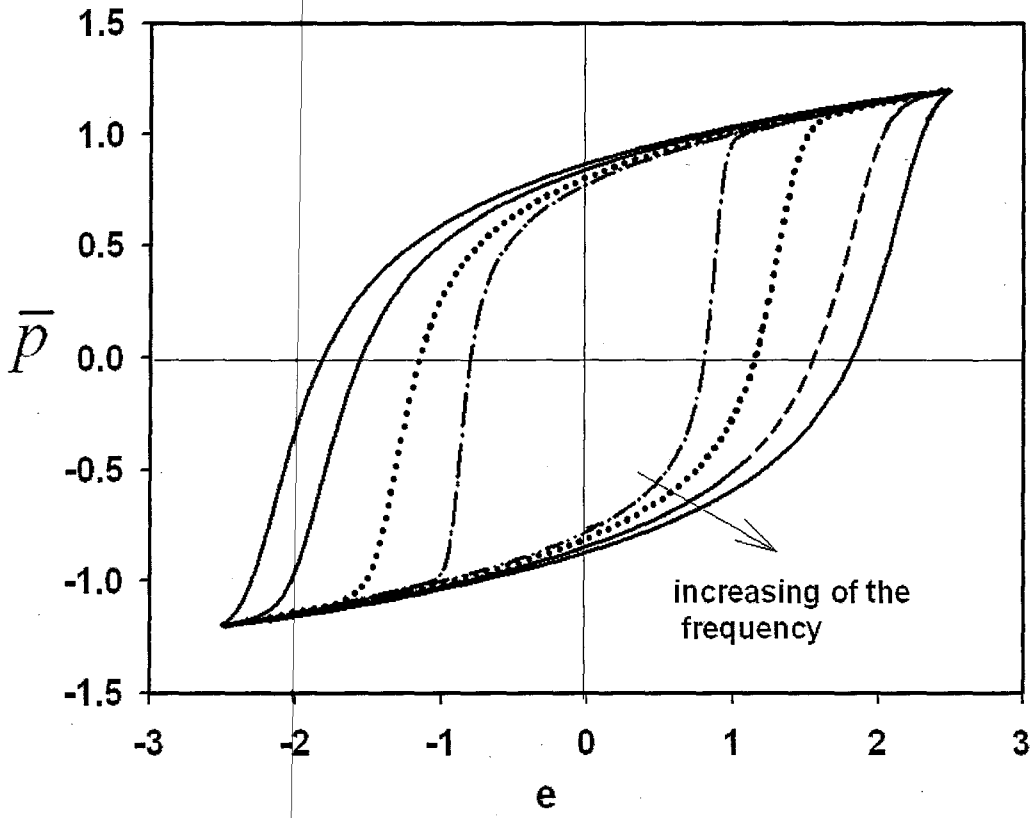


Fig. 3

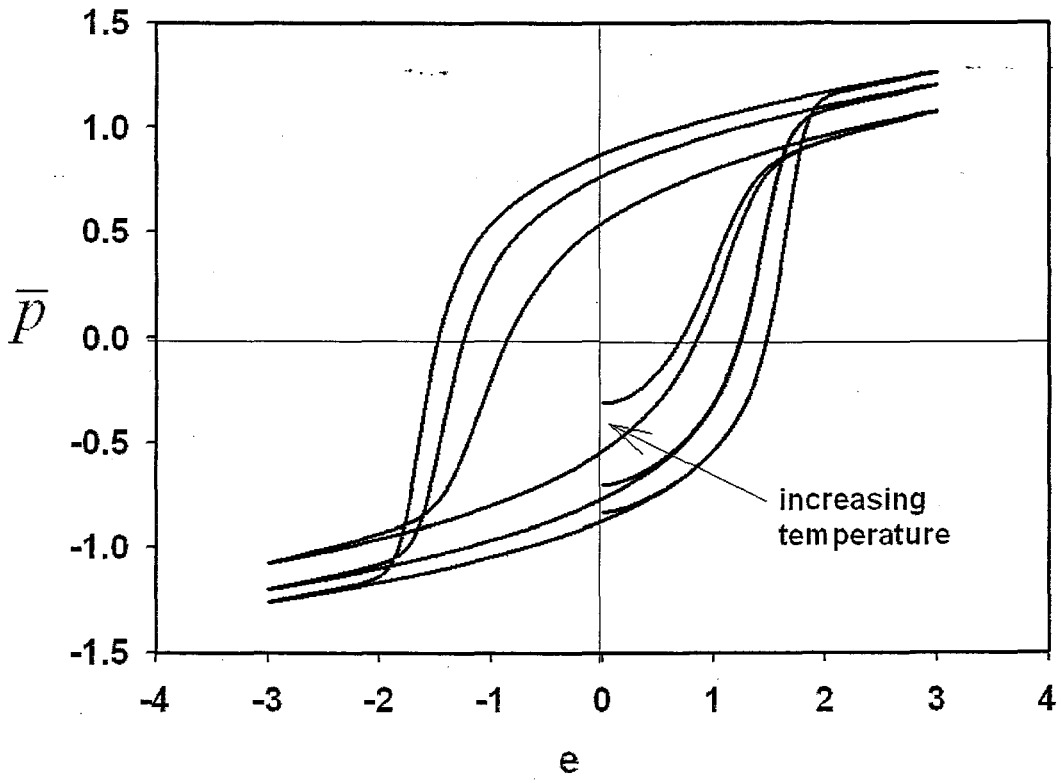


Fig. 4

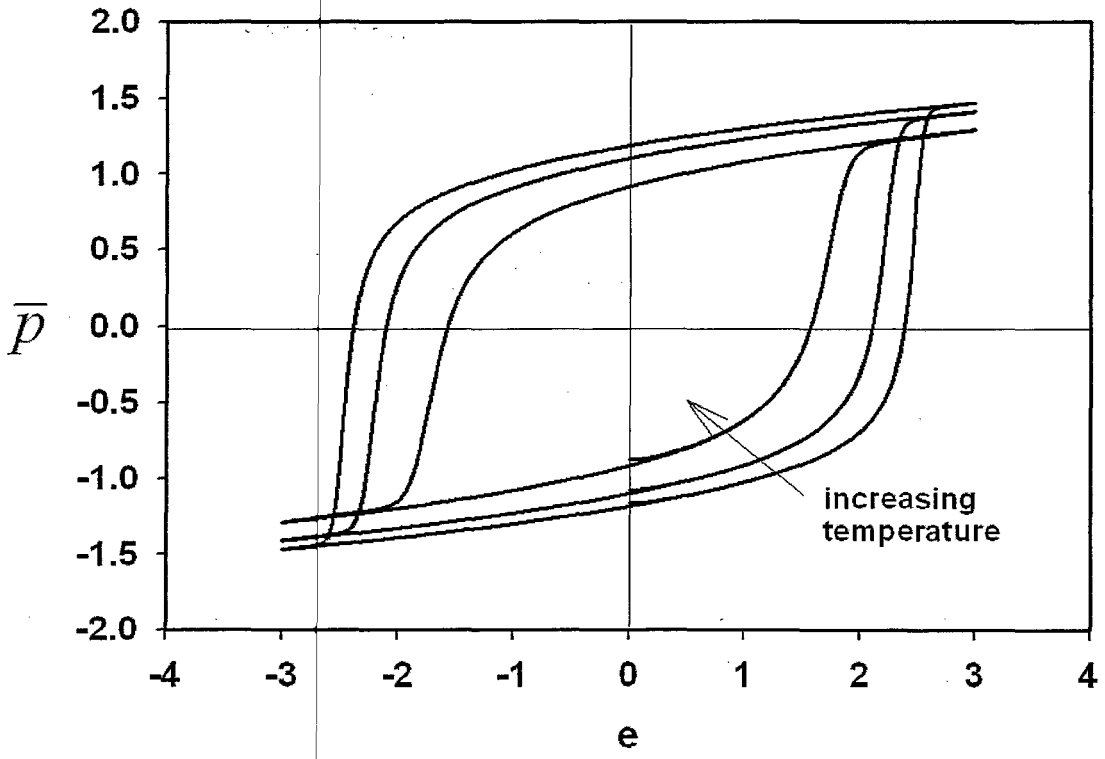


Fig. 5

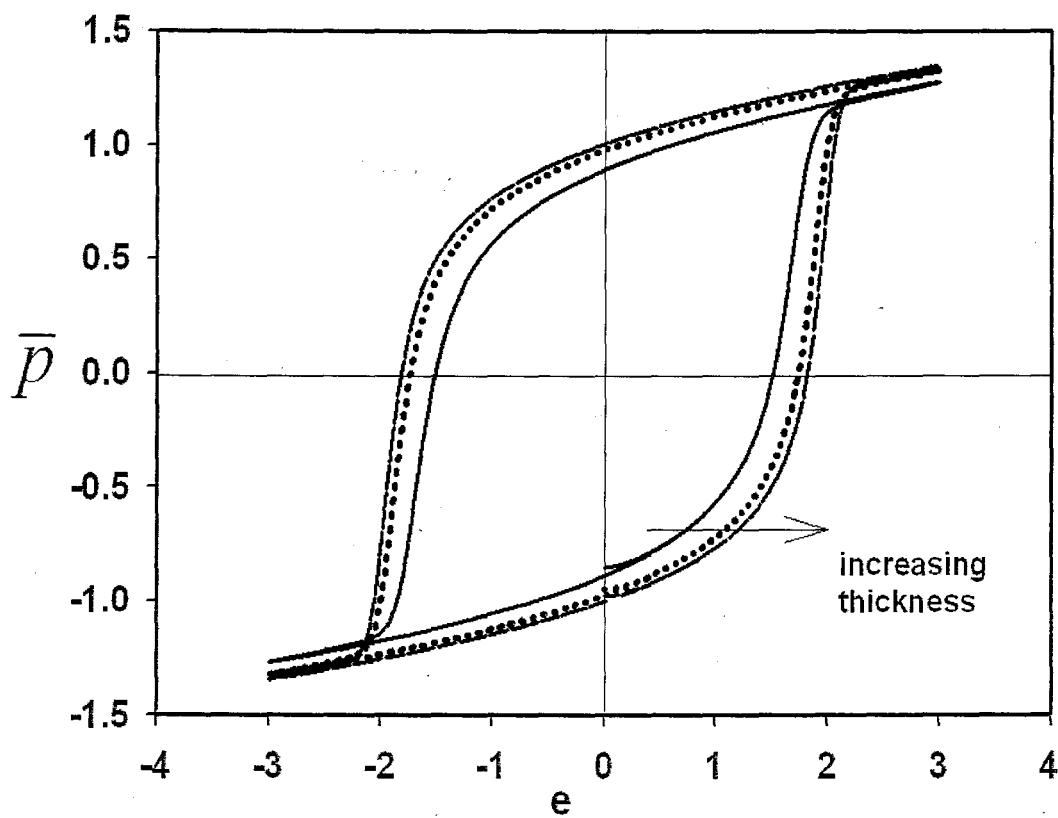


Fig. 6

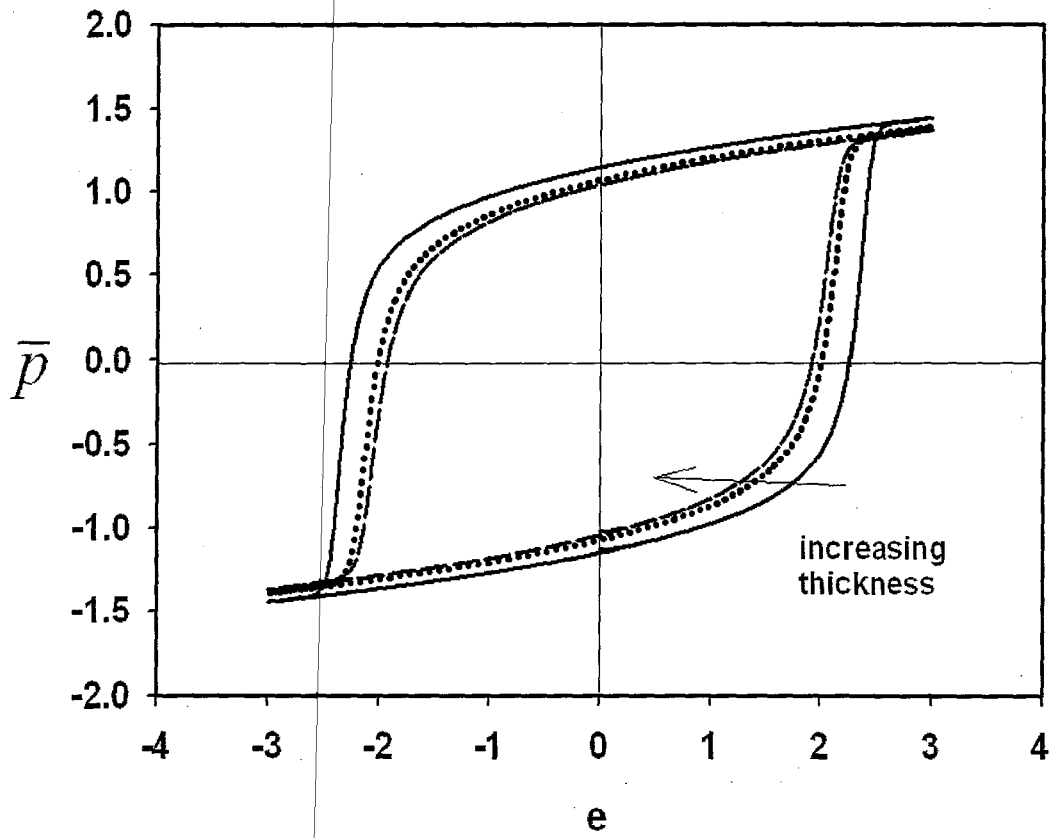


Fig. 7

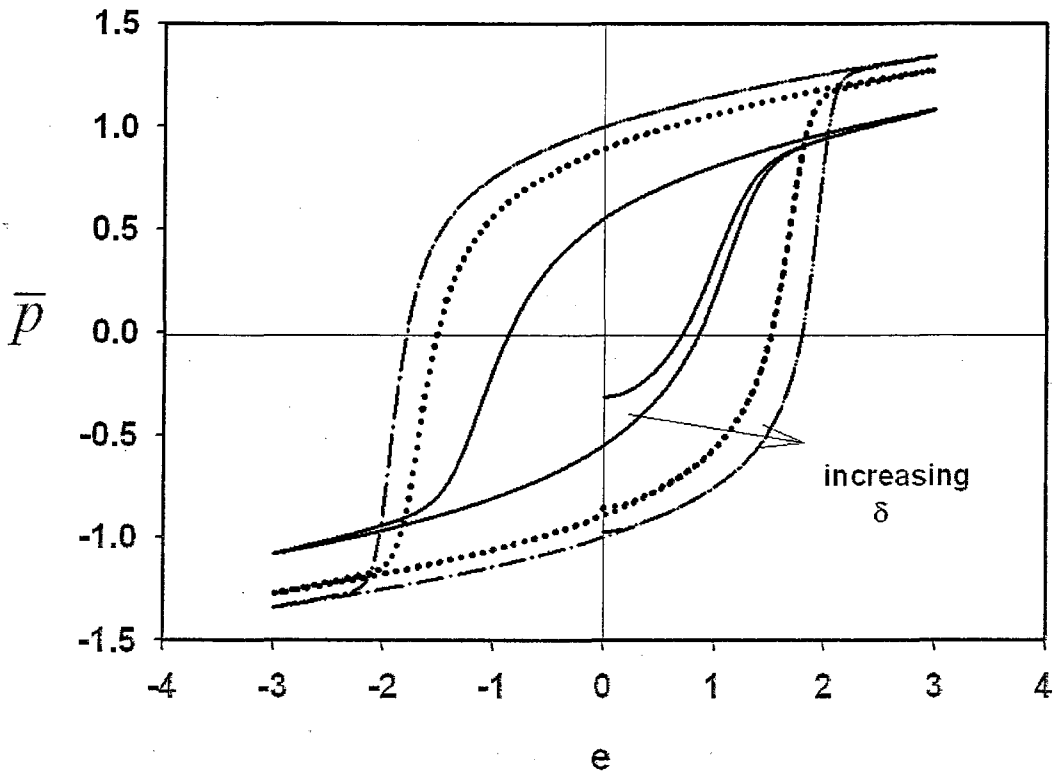


Fig. 8

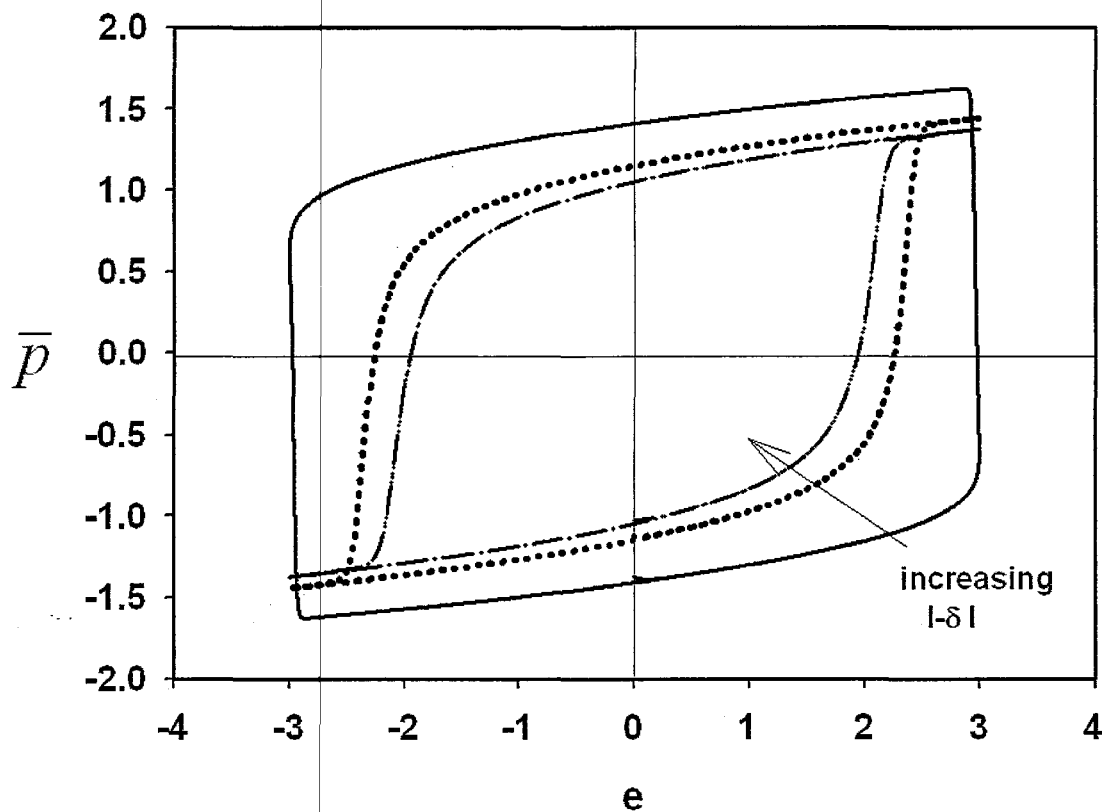


Fig. 9

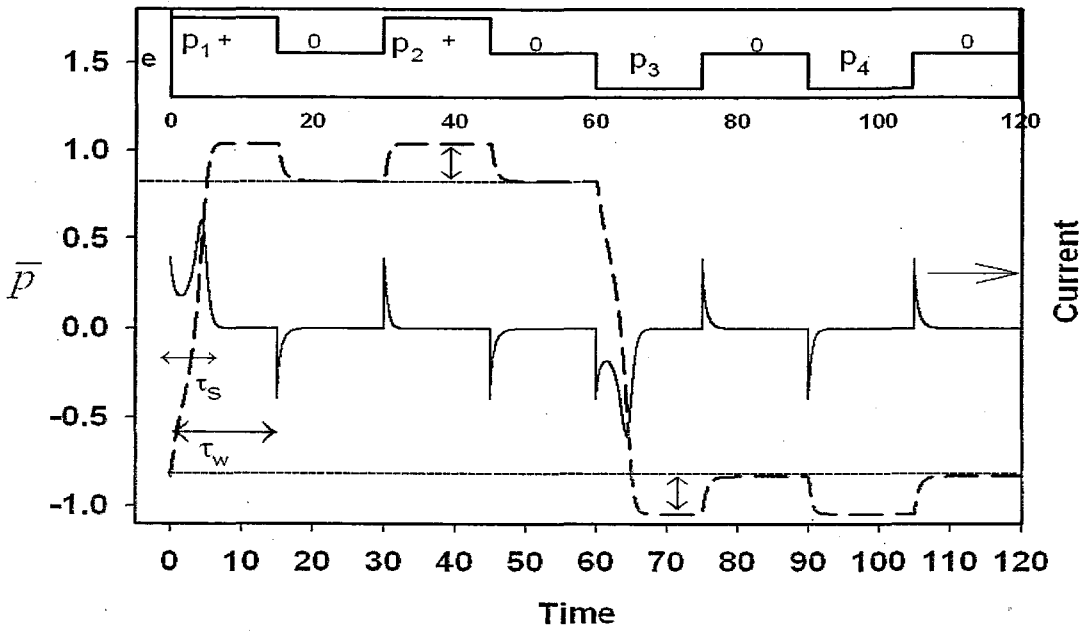


Fig. 10

	Calculated results	Experimental results
increasing amplitude $e_0$ of applied electric field	Fig. 2: $e_{cf}$ and $\bar{p}_r$ increase (Consistent with Ref. 17)	1. Ref. 16: $\bar{p}_r$ increases.
Increasing frequency $\omega$ of applied electric field	Fig. 3: $e_{cf}$ and $\bar{p}_r$ increase.	1. Ref. 18: $e_{cf}$ increases. 2. Ref. 19: $e_{cf}$ increases but $\bar{p}_r$ constant
Increasing temperature	Fig. 4 ( $+\delta_r$ ) & 5 ( $-\delta_r$ ): $e_{cf}$ and $\bar{p}_r$ decrease. (Consistent with Ref. 5)	1. Ref. 20: $e_{cf}$ and $\bar{p}_r$ decrease. 2. Ref. 21: $e_{cf}$ decreases but $\bar{p}_r$ increases and then decreases.
Increasing film thickness	Fig. 6 ( $+\delta_r$ ): $e_{cf}$ and $\bar{p}_r$ increase. (Consistent with Ref. 24) Fig. 7 ( $-\delta_r$ ): $e_{cf}$ and $\bar{p}_r$ decrease.	1. Ref. 22 & 23: $e_{cf}$ and $\bar{p}_r$ increase. 1. Ref. 25: $e_{cf}$ decreases but $\bar{p}_r$ increases. 2. Ref. 26: $e_{cf}$ decreases but $\bar{p}_r$ constant

Table 1

# Temperature and Electric Field Influences on Polarization Reversal of Ferroelectric Thin Film

Ahmad Musleh and Ong Lye Hock

*School of Physics, Universiti Sains Malaysia, 11800 USM, Penang, Malaysia*

**Abstract.** We used the Landau-Ginzburg-Devonshire (LGD) theory for a second order ferroelectric (FE) thin film modified by Tilley and Zeks which includes the energy term due to the interaction of electric field  $E$  with polarization  $P$  and with the aid of Landau Khalatnikov's dynamic equation to investigate the effects of temperature and applied electric field on polarization reversal of ferroelectric (FE) thin film. The surface parameter  $\delta$  which affects the spontaneous polarization at the film surfaces is the main feature of the model, where positive  $\delta$  causes the suppression of surface polarization and negative  $\delta$  has the reversed effect. We found that increasing the temperature tends to decrease the switching time, saturated polarization and the peak of switching current for FE films with  $\pm\delta$ . The effects of the applied electric field are reflected through the decrease in switching time and the increase of the maximum switching current as well as the saturated polarization for higher values of electric field. Our results agree with experimental results reported in the literature.

**Keywords:** Polarization reversal, Tilley-Zeks model, Electric field, Temperature

**PACS:** 77.80.Fm

## INTRODUCTION

Since the 1950's, detailed studies on the measurements of the switching characteristics of ferroelectric (FE) materials have been reported and as a consequence of those experimental results, a few theories on polarization switching have been proposed to study the switching properties of FE thin film [1-4]. All these theories ignore the surface effects on polarization reversal of FE thin films. In this paper we examine the polarization reversal of FE film by using the continuum model based on Landau free energy expression for second order FE thin film proposed by Tilley and Zeks [5] and a term  $P \cdot E$ , which gives the energy due to interaction of electric field  $E$  with polarization  $P$  is included. Couple with the Landau-Khalatnikov (LK) dynamic equation, the effects of temperature and applied electric field on polarization reversal of FE thin film are examined. The surface parameter  $\delta$ , the extrapolation length, is the main feature of the model.  $\delta$  can be either positive or negative, and it affects the spontaneous polarization at the film surfaces. We only investigate the effect of temperature  $T$  and electric field  $E$  on the reversal polarization of FE film. However, other effects such as film thickness and surface effect has been studied [6-8].

## THE MODEL

A symmetric second order FE thin film of thickness  $L$  extending along the  $z$  axis from  $-L/2$  to  $L/2$  is considered. Polarization and related physical quantities vary as a function of  $z$ . The polarization direction is normal to the film surfaces. Since we consider FE materials with finite conductivity, thus the depolarization field can be ignored [9]. LGD free energy  $F$  over a surface area  $S$  for a thin film under the influence of external electric field  $E$  has the form [5, 10]

$$\frac{F}{S} = \int_{-L/2}^{L/2} \left[ \frac{A(T-T_C)}{2\varepsilon_0} P^2 + \frac{B}{4\varepsilon_0^2} P^4 + \frac{D}{2\varepsilon_0} \left( \frac{dP}{dz} \right)^2 - EP \right] dz + \frac{D}{2\varepsilon_0 \delta} (P_-^2 + P_+^2) \quad (1)$$

All the parameters and the coefficients in the above equation are well described in refs. 5 and 10. For the purpose of numerical study, parameters are scaled as dimensionless quantities given in ref. 11. For a film, the equilibrium polarization profile  $P(z)$  corresponds to a minimum of  $F/S$ , can be obtained as a solution of the Euler-Lagrange (EL) equation following the variation of free energy in Eq. 1; and the EL equation in dimensionless form is as follows:

$$\frac{d^2 p}{d\zeta^2} = (t-1)p + p^3 - \frac{2}{3\sqrt{3}}e \quad (2)$$

The following reduced boundary conditions are obtained from variation of Eq. 1;

$$\frac{dp}{d\zeta} = \mp \frac{p}{\delta_r} \quad \text{at} \quad \zeta = \pm \frac{l}{2} \quad (3)$$

where  $\delta_r = \delta / \xi_0$ . The phenomenological Landau-Khalatnikov (LK) equation can be written in scaled form as

$$\frac{\partial p}{\partial \tau_r} = -\frac{\partial f}{\partial p} = (1-t)p - p^3 + \frac{d^2 p}{d\zeta^2} + \frac{2}{3\sqrt{3}}e \quad (4)$$

where  $f$  is the reduced energy of film given by  $f = BF / A^2 T_C^2 S \zeta_0$  and the reduced time is  $\tau_r = \tau (A T_C \zeta_0 / \varepsilon_0 \gamma)$ ; where  $\tau$  is the dimensional time. The parameter  $\gamma$  is the coefficient of viscosity. The global order parameter is the average polarization of the film which can be written as  $\bar{p} = (1/l) \int_{-l/2}^{l/2} p(\zeta) d\zeta$ , and the reduced switching current can be written as  $J_r = d\bar{p} / d\tau_r$ . The coercive field of the bulk can be obtained from the equilibrium conditions of the bulk free energy, and its reduced form is  $e_{cb} = (\sqrt[3]{1-t})^3$ . We can also find the initial polarization profile by solving the reduced form of EL

equation (Eq. 2) in zero field by Runge-Kutta (R-K) method and the form of polarization profiles must satisfy the boundary conditions set by Eq. 3. This initial polarization is used as the starting value for switching simulation, in which Eq. 4 is solved by R-K integration with finite difference method.

## RESULTS AND DESCUSSION

The polarization reversal of FE film is studied by applying step electric field  $e$  that is usually used in experiments [12]. The initial polarization in the film is switched from its negative value by a positive pulse. Figure 1 shows the evolution of average polarization  $\bar{p}$  with time for different temperature  $t$  in FE film with  $\delta_r = +3$ . By increasing the temperature  $t$ , the switching time  $\tau_s$  and the saturated polarization decrease. The inset in Fig. 1 shows the time dependence of switching current, it is obvious that by increasing  $t$ , the maximum current decreases.

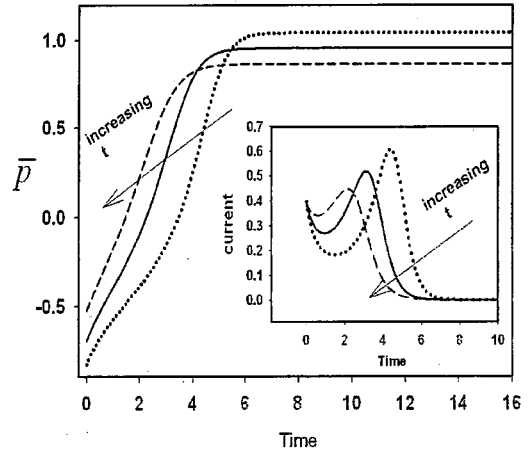


**Figure 1** Average polarization versus time for temperatures  $t = 0.0, 0.2$  and  $0.4$ .  $l = 1.8$ ,  $\delta_r = +3.0$ ,  $e = 1.0$ . The inset shows the corresponding switching current.

Experimental measurements for  $\text{BaTiO}_3$  at different temperatures show that at higher temperature,  $\tau_s$  becomes shorter [13]. Increasing  $t$  may increase the velocity of domain due to the increase in system energy, thus  $\tau_s$  decreases. Regarding the decrease in saturated polarization with increasing  $t$  in our simulation, the result is in agreement with experimental result of Yuan *et al.* [14]. The effect of temperature on FE film with  $-\delta_r$  is similar to that of the FE film with  $\delta_r$ , and it is not present here. Figure 2 shows the graph of  $\bar{p}$  versus time  $\tau_r$  for different values of  $e$  for film with  $\delta_r = +3$ . By increasing  $e$ , the FE film switches faster and  $\bar{p}$  increases. It can be seen that the initial polarization of FE thin film can be completely reversed by  $e = 0.8 e_{cb}$  (dotted curve in Fig. 1). This value of  $e$  is less than the bulk coercive field  $e_{cb}$ ,  $e_{cb} = 1$  at temperature  $t = 0.0$ . We can explain why the FE film is switched by electric field which is less than  $e_{cb}$ . For FE film with positive  $\delta_r$ , the polarization is suppressed at the surface compared with the value inside the film; and the value of polarization in the interior of the film is always lower than that of the bulk value [11, 15]. From this respect, the value of average polarization of this film is always less than the value of the bulk polarization; hence we may deduce that switching would take place more readily in the film with  $+\delta_r$ , than in the bulk for lower applied field ( $e < e_{cb}$ ). However for FE film with negative extrapolation length the coercive field is larger

than the bulk value [7]. The double dot-dashed curve in Fig. 2 is the polarization which is not completely switched by  $e = 0.5e_{cb}$  ( $e < e_{cf}$ ). The coercive field of this film is  $e_{cf} = 0.54e_{cb}$  as indicated by the arrow in the inset of Fig. 2. It is interesting to note that at  $e = 0.50e_{cb} < e_{cf}$ , only some dipoles can be reversed and it is in agreement with the results of the experiment [16]. The corresponding switching current of polarization reversal curves of Fig. 2 is shown in Fig. 3. From the curves in Fig. 3, the peak current increases with increasing  $e$  and this result is consistent with experimental reports [16].

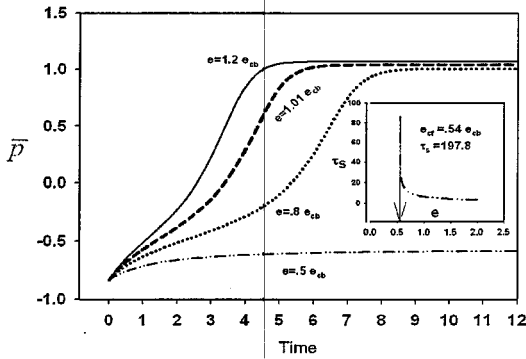


**Figure 2** Average polarization versus time for electric fields  $e = 0.5, 0.8, 1.01$  and  $1.2$ .  $l = 1.8$ ,  $\delta_r = +3.0$ ,  $t = 0.0$ . The inset shows the switching time versus applied field  $e$ . The arrow inside the inset indicates the film coercive field  $e_{cf}$ .

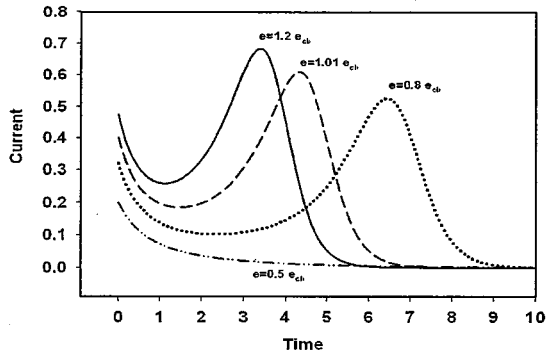


**Figure 3** Switching current versus time for  $e = 0.5, 0.8, 1.01$  and  $1.2$ .  $l = 1.8$ ,  $\delta_r = +3.0$ ,  $t = 0.0$ . This figure corresponds to the Fig. 2.

## AKNOLEDGMENT

The work is funded by the SAGA grant, Academy of Sciences Malaysia (Grant No: 304/PFIZIK/653018/A118).

## REFERENCES

1. H. Orihara, S. Hashimoto, and Y. Ishibashi, *J. Phys. Soc. Jpn.* **63**, 1031 (1994).
2. V. Shur, E. Rumyantsev, and S. Makarov, *J. Appl. Phys.* **84**, 445 (1998).
3. A. K. Tagantsev *et al.*, *Phys. Rev. B* **66**, 214109 (2002).
4. Y. Ishibashi, *J. Phys. Soc. Jpn.* **59**, 4148 (1990).
5. D. R. Tilley, and B. Zeks, *Solid State Commun.* **49**, 823 (1984).
6. L. H. Ong, and A. Musleh, *Ferroelectrics in press* (2008).
7. A. Musleh, L. H. Ong, and J. Osman, submitted to *J. Appl. Phys.* (2008).
8. A. Musleh, L. H. Ong, and J. Osman, submitted to *J. Phys.: Condens. Matter* (2008).
9. Watanabe Y., *Phys. Rev. B* **57**, 789 (1998).
10. K. Binder, *Ferroelectrics* **35**, 99 (1981).
11. L. H. Ong, J. Osman, and D. R. Tilley, *Phys. Rev. B* **63**, 144109 (2001).
12. W. J. Merz, *J. Appl. Phys.* **27**, 938 (1956).
13. W. J. Merz, *Phys. Rev.* **95**, 690 (1954).
14. G. L. Yuan *et al.*, *Materials Science and Engineering B* **118**, 225 (2005).
15. Y. Ishibashi, H. Orihara, and D. R. Tilley, *J. Phys. Soc. jpn.* **71**, 1471 (2002).
16. E. Tokumitsu, N. Tanisake, and H. Ishiwara, *Jpn. J. Appl. Phys.* **33**, 5201 (1994).

# Effects of Compressive Stress on Ferroelectric Epitaxial Films

Ahmad Musleh, Lye-Hock Ong\*, Junaidah. Osman

School of Physics, Universiti Sains Malaysia, 11800 USM, Penang, Malaysia.

**Abstract.** A one dimensional Landau-Devonshire model is used to study the misfit strain,  $S_m$ , dependent of phase transition in a single domain Ferroelectric barium titanate (BT) epitaxial films. These films are usually grown on thick cubic substrates, thus, imposing biaxial compression in the film plane. It is found that the phase transition of the strained BT thin films becomes second order in spite of the fact that the phase transition of stress-free BT films is first-order. The ferroelectric properties of strained BT are enhanced remarkably by the induced stress. We have found that the spontaneous polarization of strained BT with thicknesses  $< 9$  nm is higher than the spontaneous polarization of stress-free BT bulk for long ranged negative misfit strain  $S_m < -7 \times 10^{-3}$ , though the stress-free BT films have no ferroelectricity for thicknesses less than 9 nm. Here, we compare our results with the available experimental data.

Key words: Landau Theory, barium titanate, strain.

PACS: 77.84.Dy; 77.65.Ly

## INTRODUCTION

Ferroelectric epitaxial films are required for the electro-optic applications as optical wave guide due to their low propagation loss [1]. Epitaxial films of ferroelectric barium titanate (BT) grown on much thicker substrates have been studied experimentally for a long time [2, 3]. Pertsev *et al.* [4] have developed a thermodynamic theory of ferroelectric BT thin film epitaxially grown on cubic substrates using the sixth-order polynomial for Landau-Devonshire (LD) potential with the temperature-dependent coefficients taken from ref. 5. However, the LD potential is only applicable to BT films under relatively small compressive strain ( $\leq 0.6\%$ ). It has been shown experimentally that BT thin film may be subjected to much higher compressive strain (2.6%) [2, 3]. For this reason we adopt an eighth-order polynomial term for the LD potential with new LD coefficients developed by Li *et al.* [6] to study the polarization properties of strained epitaxial ferroelectric BT films. The intrinsic effect of the film surfaces on the spontaneous polarization is taken into account via the concept of extrapolation length,  $\delta$  with positive value.

## A Phenomenological Thermodynamic

We consider a symmetric epitaxial thin film of BT of thickness,  $L$  extended along the  $z$ -axis, which is grown in a high-temperature paraelectric state on a thick (001) cubic substrate. The thick substrate induces biaxial compressive stress in the  $x$ - $y$  plane of the film. The spontaneous polarization  $P_s$  orthogonal to the substrate surface is expected to be stable with the stability condition,  $S_m < S_m^0(T) = Q_{12}P_0^2(T)$  for tetragonal  $c$ -phase [7], where  $S_m$  is the misfit strain,  $Q_{12}$  is the electrostrictive constant and  $P_0(T)$  is the spontaneous polarization of a stress-free crystal. We consider that the model is one dimensional with  $P_s$  and the other related quantities vary as a function of  $z$  (in tetragonal  $c$ -phase). We assume that the film is sandwiched between two extended identical electrodes in short-circuited condition, where depolarization field is neglected for BT due to its finite conductivity [8]. The elastic field is

assumed to be homogeneous in the film and any changes on the surface of the substrate due to contribution of strain gradient is neglected for improper ferroelectric BT perovskite. Under these physical conditions the LD free energy per unit area of BT thin film including the eighth-order polynomial term for the film of thickness  $L$  in tetragonal  $c$ -phase can be rewritten as follow [9]:

$$G_f/A = \int_{-L/2}^{L/2} \left[ \tilde{G}(z) + \frac{1}{2} g \left( \frac{dP}{dz} \right)^2 \right] dz + G_s; \quad (1)$$

where,  $\tilde{G}$  is the energy of the modified thick film given by [4, 6]:

$$\tilde{G} = A^*P^2 + B^*P^4 + CP^6 + DP^8 - EP + \frac{S_m^2}{s_{11} + s_{12}}. \quad (2)$$

All coefficients  $A^*$ ,  $B^*$ ,  $C$ ,  $D$  and  $s_{ij}$  are defined as in ref. 4 and ref. 6. Finally  $G_s$  is the surface energy contribution of the film, given by [10]:

$$G_s = \frac{1}{2} g \delta^{-1} (P_-^2 + P_+^2), \quad (3)$$

where  $P_-$ ,  $P_+$  are the polarization values at the film surfaces at  $z = \mp L/2$ . Minimization of the functional in Eq. 1 leads to the Euler-Lagrange equation

$$g \frac{d^2P}{dz^2} = 2A^*P + 4B^*P^3 + 6CP^5 + 8DP^7 \quad (5)$$

with the following boundary conditions

$$\frac{dP}{dz} = \pm \frac{P}{\delta} \quad \text{at} \quad z = \mp L/2 \quad (6)$$

The adopted values of the gradient coefficient,  $g = 2.7 \times 10^{-9} \text{ J.m}^3/\text{C}^2$  and the extrapolation length,  $\delta = 6.56 \times 10^{-9} \text{ m}$  for size and surface effects are taken from ref. 11 and ref. 12 respectively.

The polarization profile  $P(z)$  is found by solving Eq. 5, using the 4<sup>th</sup> order Runge-Kutta (R-K) method, subjected to the boundary conditions set by Eq. 6. The global order parameter is the average polarization of the thin film defines as

$$\bar{P} = \frac{1}{L} \int_{-L/2}^{L/2} P(z) dz \quad (7)$$

## Results and Analysis

The average polarization,  $\bar{P}$  versus temperature is plotted as shown in Fig.1 for thick (dashed, dot-dashed curves) and thin (solid curves) films. It is obvious that the eighth-order potential with the new coefficients [6] shows a well-behaved second order ferroelectric phase transition. Note that the phase transition for stress-free bulk crystal of BT is first-order (dotted curve). By increasing the misfit strain,  $S_m$ , the transition temperature,  $T_c$  and  $\bar{P}$  increase remarkably for thick film.  $T_c$  of thin films still above the transition temperature of the stress-free bulk even for strained ultra thin film with thickness  $L = 6$  nm. Film with thickness  $L = 6$  nm has  $\bar{P}$  close to the stress-free bulk in spite of this film thickness has no ferroelectric phase under stress-free condition as shown in Fig.2. The thickness dependence of

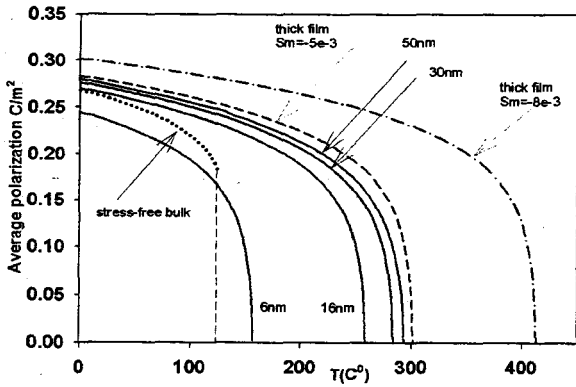


FIGURE 1. The average polarization,  $P_s$  versus temperature for thick strained BT films (dashed and dot dashed curves) under misfit strains,  $S_m = -5 \times 10^{-3}$  and  $S_m = -8 \times 10^{-3}$  respectively. The solid curves are thin films with various thicknesses in nanometre (nm) under  $S_m = -5 \times 10^{-3}$ . The dotted curve is for stress-free bulk.

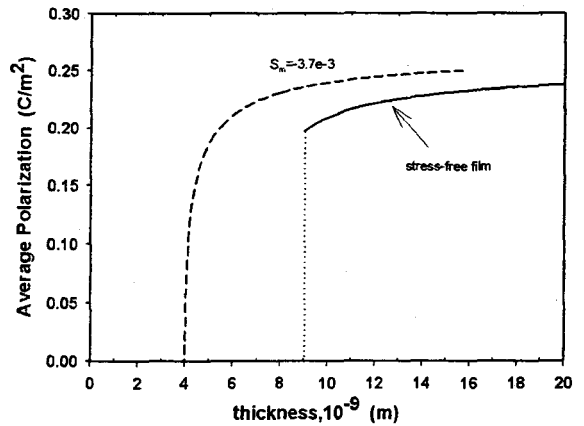
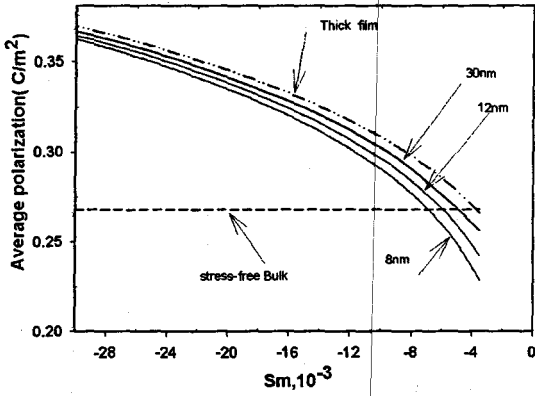
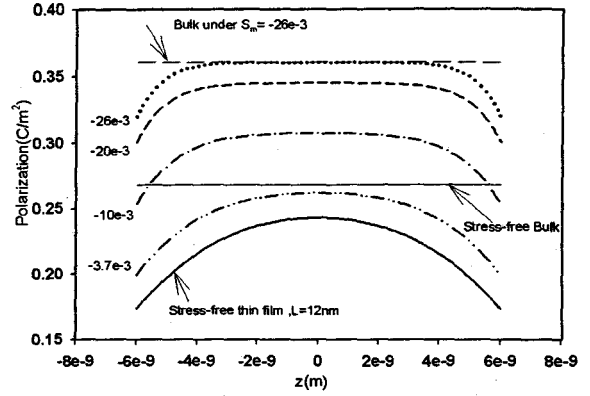


FIGURE 2. Average polarization versus temperature. Solid curve is for the stress-free BT film and the dashed curve is for the strained BT film at  $S_m = -3.7 \times 10^{-3}$

the polarization for BT strained films at room temperature,  $T = 25^\circ C$ , shows that the polarization of strained film approaches zero continuously in Fig. 2. This is a characteristic of second-order phase transition and the same phase transition is also shown in the temperature dependence of the polarization in Fig.1. From Fig. 2, it can be seen that the critical thickness where the polarization disappears is 4 nm at  $S_m = -3.7 \times 10^{-3}$ ; whereas the critical thickness for the stress-free film is 9 nm (solid curve). The effect of substrate compression upon the average spontaneous polarization of various thicknesses of BT films at room temperature is shown in Fig.3. It is obvious that for a wide range of negative misfit strain  $S_m < -7 \times 10^{-3}$  due to strong biaxial compression from the substrates, the polarizations are above the spontaneous polarization  $P_s = 0.2682 C/m^2$  of free crystal even at ultra strained thin film of thickness,  $L = 8$  nm where ferroelectricity is expected to disappear for stress-free film of BT at thickness  $L = 9$  nm as shown in Fig.2.



**FIGURE 3.** Misfit dependence of average polarisation for different thicknesses (nm) of strained BT films. Dashed line is the spontaneous polarization of stress-free bulk



**FIGURE 4.** Polarization profile  $p(z)$  versus  $z$  for strained BT film with thickness  $L = 12$  nm under various strain as indicated. Solid curve is for stress-free BT film with  $L = 12$  nm, solid straight line is for stress-free bulk and long-dashed line for strained bulk BT.

Recently Kim *et al.* [3] have prepared high-quality epitaxial BT films using pulsed laser deposition with in-situ reflection high-energy electron diffraction. For epitaxial BT film with misfit strain of  $S_m = -26 \times 10^{-3}$ , their observed value of remnant polarization,  $P_r$  with thickness,  $L = 30$  nm is about  $0.36 C/m^2$ , while our theoretical prediction is  $0.357 C/m^2$ ; which is highly in agreement with their measurement. Another comparison can be made with the experimental data of Yanasa *et al.* [2], where their epitaxial BT films are prepared by radio-frequency magnetron sputtering. Their reciprocal lattice mapping of the X-ray intensity reveals that BT films have almost the same  $a$ -axis as the  $SrTiO_3$  substrate for film thicknesses between 12-39 nm at misfit strain,  $S_m = -26 \times 10^{-3}$ . Their observed remnant polarization,  $P_r$  with thickness  $L = 12$  nm is about  $0.335 C/m^2$ , where our calculated value is  $0.355 C/m^2$ ; which is in fair agreement with their measurement.

Fig. 4 shows the polarization profile,  $P(z)$  of strained BT film with thickness  $L = 12$  nm for various values of misfit strain  $S_m$ . The polarizations at the surfaces are suppressed for various values of misfit strain  $S_m$ ; and this is due to the effect of positive surface extrapolation length,  $\delta$ . The polarization of the strained film under  $S_m = -20 \times 10^{-3}$  of thickness  $L = 12$  nm is greater than that of the stress-free bulk (straight solid line). However, the polarization of this film is less than that of the stress-free bulk at lower strain value of  $S_m = -3.7 \times 10^{-3}$  (double dot-dashed curve); but it is still greater than the polarization of the stress-free film of the same thickness (solid curve). Obviously the polarization at the centre of the strained film under high strain value of  $S_m = -26 \times 10^{-3}$  (dotted curve) becomes flat and it approaches the strained bulk (long-dashed curve) value.

To emphasize the phase transition of the strained BT films from ferroelectric phase to paraelectric phase is second-order is to look at the graph of entropy,  $\sigma$  versus temperature. Fig.5 shows that the entropy is continuous at the transition temperature; so the latent heat  $\Delta Q = T_C(\Delta\sigma)_{T=T_C}$  equals zero indicates the characteristic of second-order phase transition. Fig.6 shows comparison of the temperature dependence of polarizations at the surface and at

the centre of the film. It is clear that the polarization at the film-centre is greater than that at the surface over the range of temperature shown; and the polarization of the whole film is zero at transition temperature as it is expected.

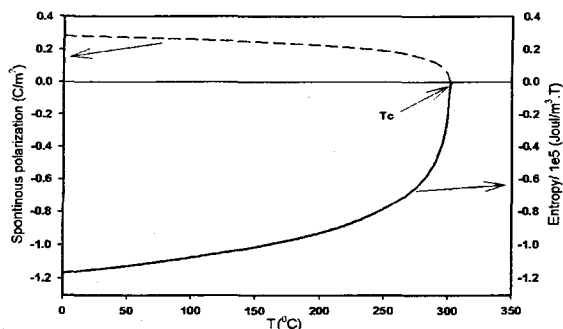


FIGURE 5. The entropy (solid curve) and average polarization (dashed curve) versus temperature for thick film of strained BT with misfit strain  $S_m = -5 \times 10^{-3}$ .

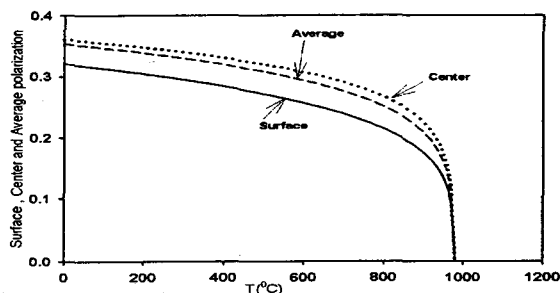


FIGURE 6. The spontaneous polarization at surface, at centre of the film and average polarization for  $L = 8$  nm under  $S_m = -26 \times 10^{-3}$

## ACKNOWLEDGEMENTS

The work is funded by the SAGA grant, Academy of Sciences Malaysia (Grant No: 304/PFIZIK/653018/A118).

## REFERENCES

- 1 M. Dawber, K. M. Rabe and J. F. Scott, *Rev. Modern physics* **77**, 1083 (2005).
- 2 N. Yanase, K. Abe, N. Fukushima and T. Kawakubo, *Jpn. J. Appl. Phys.* **38**, 5305 (1999).
- 3 Y. S. Kim, D.H. Kim, J. D. Kim and Y. J. Chang, *App. Phys. Letter*, **86**, 102907 (2005).
- 4 N. A. Pertsev, A. G. Zembilgotov, and A. K. Tagantsev, *Phys. Rev. Lett.* **80**, 1988 (1998).
- 5 A. J. Bell and L. E. Cross, *Ferroelectrics*, **59**, 197 (1984).
- 6 Y. L. Li, L. E. Cross and L. Q. Chen, *J. Appl. Phys.* **98**, 064101(2005).
- 7 N. A. Pertsev, and V. G. Khoukhar, *Phys. Rev. Lett.* **84**, 3722 (2000).
- 8 Y. Watanabe, *Phys. Rev. B* **57**, 789 (1998).
- 9 K. Binder, *Ferroelectrics* **35**, 99 (1981).
- 10 R. Kretschmer and K. Binder, *Phys. Rev. Lett.* **20**, 1065 (1979).
- 11 A. G. Zembilgotove, N. A. Pertsev, H. Kohlstedt and R. Waser, *J. Appl. Phys.* **91**, 2247 (2002).
- 12 W. L. Zhong, B. D. Qu, P.L. Zhang and Y. G. Wang, *Phys. Rev. B* **50**, 12375 (1994).

# Switching Behaviours of Ferroelectric Films for Fixed and Free Surface Boundary Conditions

Lye-Hock Ong<sup>\*1</sup>, Ahmad Musleh<sup>1</sup>, J. Osman<sup>1</sup>, and Y. Ishibashi<sup>2</sup>

<sup>1</sup>School of Physics, Universiti Sains Malaysia, 11800 USM, Penang, Malaysia.

<sup>2</sup>Faculty of Business, Aichi Shukutoku University, Nagakute-cho, Aichi, Japan.

Key words: Landau Theory, polarization reversal, surface effect, size effect

*\*Corresponding author, E-mail address: onglh@usm.my*

We present a study on the switching behaviours of ferroelectric films based on Landau free energy expression for fixed and free surface boundary conditions in ferroelectric films. General switching phenomena are observed from the results of both models. However, the delay in switching at the centre of the film relative to switching near the surface for fixed surface boundaries is more remarkable as the film thickness increases. It is predicted by both models that dipole moments at the centre and near the surface switch almost together in thin films. Results obtained from the free surface boundary show that the surface extrapolation length  $\delta$  influences the coercive field and the critical thickness of the film.

## Introduction

Theoretical and experimental studies on switching behaviours in ferroelectric (FE) materials began a long time ago [1, 2]. Since the past couple of decades, the interest in switching behaviours of FE thin films has been rekindled due to the advancement in thin film fabrication technology, where higher quality and more reliable FE thin films can be fabricated; thus making applications of FE thin films in microelectronic devices and memories [3 – 5] more reliable. The renewed interest in FE thin films, both theoretically and experimentally, is focused more on elucidation of phenomena such as size and surface effects on switching time and coercive field [6 – 11] in polarization reversal of FE thin films. From the perspective of theory, several models based on a Landau-typed phase transition have explained well on the switching behaviours of mesoscopic ferroelectric structures [7, 9]; and some of the predictions concerning size and surface effects on switching behaviours by

Landau-typed models agree well with experimental observations. However, there is still lacking of detailed understanding on the effect of applied electric field at the surfaces which is very important to the global understanding on the behaviours of polarization reversal in the film as a whole. In this paper, we adopt the discrete model of Landau Devonshire (LD) free energy expansion for a one dimensional FE film whereby a 'surface term' is introduced in the free energy in an applied electric field [12]. With this framework, we present the results of switching behaviours of FE film with fixed and free surface boundary conditions.

### Theoretical Model

Recently, Chew *et al.* [13] have presented a study on polarization reversal of FE films using the LD model; and they just consider the effect of applied electric field  $E$  on the film interior but not on the surfaces. However, when an electric field is applied to a film, the surfaces should feel the same electric field as in the interior; so it is natural to consider the energy due to the electric field at the surfaces, especially when the applied electric field is large in the dynamic studies of polarization reversal of FE films. Assuming that the one-dimensional FE film is made up of  $2N$  cells with  $+N^{\text{th}}$ -cell and  $-N^{\text{th}}$ -cell are at the surfaces of the film. We assign the terms of polarization at the  $i^{\text{th}}$ -cell in the film interior and at the surfaces as  $p_i$  and  $p_{\pm N}$  respectively. The average free energy of the FE film under the applied field  $E$  in a discrete form in terms of the polarization can be written as [12]

$$F = \frac{1}{2Na} \left[ a \sum_{i=-(N-1)}^{N-1} f_i + a \sum_{i=-(N-1)}^{N-1} f_{\text{int}} + a(f_N + f_{-N}) \right] \quad (1)$$

where  $f_i$  is the local potential density of the  $i^{\text{th}}$ -cell in the interior which can be expressed as

$$f_i = \frac{\alpha}{2} p_i^2 + \frac{\beta}{4} p_i^4 - p_i E, \quad (2)$$

where  $\alpha$  and  $\beta$  are constants as usual, and  $E$  the applied field. The energy of the surfaces at  $i = \pm N$  is of the form

$$f_{\pm N} = \frac{k_{\pm}}{2} p_{\pm N}^2 - p_{\pm N} E, \quad (3)$$

where the thickness of the surface is assumed to be one lattice unit, and  $k_{\pm}$  are constants.

Finally,  $f_{\text{int}}$  represents the interaction energy between the neighbouring cells,

$$f_{\text{int}} = \frac{\kappa}{2} \left( \frac{p_{i+1} - p_i}{a} \right)^2, \quad (4)$$

where  $a$  is the lattice constant and  $\kappa > 0$ ,

It has been shown in ref. 12 that the free energy in the discrete form in (1) can be transformed into the continuum form, in terms of a continuous variable  $p(z)$  as

$$F = \frac{1}{L} \left\{ \int_{-L/2}^{L/2} \left[ \frac{\alpha}{2} p^2 + \frac{\beta}{4} p^4 - pE + \frac{\kappa}{2} \left( \frac{dp}{dz} \right)^2 \right] dz + \frac{\kappa}{2\delta_+} p_+^2 - ap_+ E + \frac{\kappa}{2\delta_-} p_-^2 - ap_- E \right\}. \quad (5)$$

Equation (5) represents the average free energy of a symmetric second-order FE thin film of thickness  $L$ , where  $L$  can be related to  $2N$  times the lattice constant  $a$ , under an applied field  $E$ . To minimize  $F$  with respect to the continuous variable  $p(x)$ , we have to solve the Euler-Lagrange (EL) equation

$$\alpha p + \beta p^3 - E - \kappa \frac{d^2 p}{dz^2} = 0. \quad (6)$$

with the boundary conditions at  $z = L/2$  and  $z = -L/2$  as

$$\left. \frac{dp}{dz} \right|_+ = - \left( \frac{p_+}{\delta_+} - \frac{a}{\kappa} E \right), \quad (7)$$

and

$$\left. \frac{dp}{dz} \right|_- = \frac{p_-}{\delta_-} - \frac{a}{\kappa} E, \quad (8)$$

respectively. From ref. 12 also, it has been shown that the second terms in the right hand side of (7) and (8) come from the surface layer of finite thickness, and so we can call them the surface thickness related terms. We will now use the average free energy function in (1) as the framework to describe the behaviours of FE film with free surface boundary. When the applied field exceeds its coercive field  $e_c$ , the polarizations at the surfaces as well as the interior will be reversed.

On the other hand, for the FE film with fixed surface boundary, we assumed the polarizations at the film surfaces to be pinned at zero value and hence there is no switching at the surfaces. This assumption which associates with pinning of dipole moments at surfaces of non-ferroelectric sites is physical and can be realized experimentally. However, (1) has to be modified by putting  $p_{\pm} = 0$  to accommodate the assumed zero surface polarizations; and as a result, it gives the average free energy of the fixed surface boundary film as

$$F = \frac{1}{L} \int_{-L/2}^{L/2} \left[ \frac{\alpha}{2} p^2 + \frac{\beta}{4} p^4 - pE + \frac{\kappa}{2} \left( \frac{dp}{dz} \right)^2 \right] dz. \quad (9)$$

To simulate its static equilibrium polarization profile, a starting equation is required; and a cosine function of the form [14]

$$p(z) = \alpha \cos\left(\frac{\pi z}{L}\right) \quad (10)$$

is chosen.

### Numerical calculations

For the purpose of numerical calculations, we will resort to the discrete formulations. For the studies of polarization reversal for low frequencies, the Landau-Khalatnikov (LK) equation of motion omitting the kinetic term as shown below is used.

$$\gamma \frac{\partial P}{\partial T} = -\frac{\delta F}{\delta P} \quad (11)$$

where  $\gamma$  is the viscosity coefficient. The discrete form of dimensionless LK equations of motion can be written for the interior and surfaces as follow:

$$\frac{\partial p_i}{\partial \tau} = (1-t)p_i - p_i^3 + \frac{1}{(\Delta\zeta)^2} (p_{i+1} - 2p_i + p_{i-1}) + \frac{2}{3\sqrt{2}} e \quad (12)$$

for the interior, and

$$\frac{\partial p_N}{\partial \tau} = -\left(\frac{1}{\Delta\zeta\delta_r}\right)p_N - \frac{1}{(\Delta\zeta)^2} (p_N - p_{N-1}) + \frac{2}{3\sqrt{3}} e \quad (13)$$

$$\frac{\partial p_{-N}}{\partial \tau} = -\left(\frac{1}{\Delta\zeta\delta_r}\right)p_{-N} + \frac{1}{(\Delta\zeta)^2}(p_{-N+1} - p_{-N}) + \frac{2}{3\sqrt{3}}e \quad (14)$$

for the surfaces respectively. Here, the parameters are scaled to the usual way; where  $p_i$  and  $p_{\pm N}$  are the dimensionless polarizations in the interior and at the surfaces respectively;  $\delta_r$  and  $\Delta\zeta$  are the dimensionless length scales for extrapolation length and lattice constant; and  $\tau$  and  $e$  are the dimensionless time and the applied electric field respectively. Thus, the dimensionless polarization current is  $i = \frac{dp}{d\tau}$ . For the free surface boundary model, polarizations at the film surfaces are influenced by the extrapolation length  $\delta$  and the surface layer term during switching. Numerical process in simulation of switching profiles in both cases of surface boundary conditions requires a static polarization profile as initial value for LK equation when an electric field  $e$  ( $e > e_{cf}$ ) is applied. For the free surface boundary films, LK Equations in (12), (13) and (14) are used to simulate the profiles of polarization during switching. The starting static profile requires in this case is obtained from solving the discrete form of EL equation and the boundary conditions. Nevertheless, equation in (12) will be sufficient to describe the dynamics of switching in fixed surface boundary film by using cosine function in (10) as initial value of (12).

The applied electric field used in the simulation takes the form of step function in reduced units as

$$e = e_0\theta(\tau) \quad (15)$$

where  $e_0$  is the amplitude, for  $e_0 = 1$  gives the equivalent of the zero-temperature bulk coercive field  $e_c$  and  $\theta(\tau)$  is the usual step function.

## Results and Discussion

Various stages of switching profiles for fixed and free surface boundary films are shown in Fig. 1 and Fig. 2 respectively for temperature  $t = 0.5$ . The starting equilibrium polarization profiles in both cases (Fig. 1 and Fig. 2) are set at negative at time  $\tau = 0$ ; and the profiles are switched by a positive applied electric field  $e$  described in (15) until it is completely saturated at  $\tau = \tau_s$ .  $\tau_s$  is the switching current, and it is defined as the time taken for the polarization current to decline to 10% of its maximum value [7, 15].

The general trend in polarization reversal of a film with fixed surface boundaries (Fig. 1 (a), (b) and (c)) shows clearly that switching time  $\tau_s$  is longer as the film gets thicker. Fig. 1 (a) ( $l = 4.5$ ) shows the switching profiles of a thinner film of fixed surface boundary where all parts of the profile are shown to switch almost together, except at the surfaces where the sites are non-ferroelectric. There is not much difference in the switching speed between regions near the surface and the interior of the film. In thicker film ( $l = 10.0$ ), the reversal of polarization begins near the surfaces first then goes on to the centre, as shown in Fig 1 (b). The sites adjacent to the surfaces are weak induced ferroelectricity that makes the region near the surfaces easier to switch than the other inner sites. This leads to domain wall formation near the surfaces, followed by domain wall movement towards the centre. Hence, when the film becomes thicker ( $l = 15.0$ ), the delay in switching at the centre portion of the film is more distinct compared with that nearer the film surfaces and it is more obvious in Fig 1 (c). In term of domain wall movement in the film, it obviously takes a longer time for a domain wall to move from the surface to the centre for a thick film than a thin film. It can be seen that the delay in switching at the centre in a fixed surface boundary film is more remarkable when the film becomes thicker.

Fig 2 (a) shows the switching profiles of a thin film ( $l = 4.5$ ) of free surface boundary where the profiles are move almost parallel to each other in the whole duration of switching. When the film gets thicker, there is obvious difference in switching between the surfaces and the centre; the dipole moments at the surfaces are switched first than that at the centre of the film (in Fig 2 (b)); and it is clearly reflected in the graph of polarization current verses time in Fig. 3. In general, switching time  $\tau_s$  is also longer as the free surface boundary film becomes thicker.

Fig. 4 shows the thickness transition of coercive field  $e_c$  for fixed and free surface boundary conditions. For free surface boundary film, the extrapolation length  $d$  has great effects on the coercive field  $e_{cf}$  and critical thickness  $l_c$  of a film. The critical thickness  $l_c$  decreases with increasing value of  $d$  as it is predicted [16]; while the coercive field  $e_{cf}$  increases with the value of  $d$ . As for a FE film with larger  $d$ , surface pinning is weak, resulting in a larger surface polarization. Consequently, a larger field is required to reverse the more energetic dipoles. On the other hand, fixed surface boundary films correspond to

films with non-ferroelectric sites at the surfaces. There is weak induced ferroelectricity at sites adjacent to the surfaces; and weak dipole moments require smaller field to switch. Hence, it explains for the shorter switching time in fixed surface boundary film than in free surface boundary film of the same thickness. It has been shown in ref. 14 that the possible range of  $d$  is  $\delta \geq 0$  and  $\delta < -a$ . From Fig. 4 it can be seen that if  $\delta \rightarrow 0$  in the free surface boundary film, the ' $d$ ' curve will approach the curve of fixed surface boundary film. Thus, the fixed surface boundary model is in fact equivalent to the free surface boundary model when  $d = 0$ .

### Conclusion

We study the effects of surface boundary conditions on switching behaviours of FE films by using the discrete LD model which includes a surface energy term in applied electric field. It has been shown that switching at the surface and at the centre is almost the same in thin FE films irrespective of fixed or free surface boundaries. For thicker films, surface switching takes place relatively earlier than the interior of the films both in free and fixed surface boundaries. However, the delay in switching at the centre is more remarkable in the fixed surface boundary films as the film thickness increases. The general trend of increasing switching time  $\tau_s$  with increasing thickness  $l$  has been seen in both cases of surface boundary conditions.

### References

- [1] W. J. Merz, Phys. Rev. **95**. 690 (1954).
- [2] E. Fatuzzo and W. J. Merz, in *Ferroelectricity*, 1<sup>st</sup> ed. Edited by E. P. Wohlfarth (Wiley, New York, 1967), Vol. 7, Chap. 1, p. 5.
- [3] J. F. Scott, *Ferroelectric Memories* (Springer-Verlag, Berlin, 2000)
- [4] H. Uchida, N. Soyama, K. Kageyama, K. Ogi, and C. A. Paz de Araujo, Integr. Ferroelectr. **8**. 41 (1997)
- [5] C.S. Ganpule, S. Stanishevsky, Q. Su, S. Aggarwal, J. Mengailis, E. Williams, and R. Ramesh, Appl. Phys. Lett. **75**. 409 (1999)
- [6] T. Hase and T. Shiosaki, Jpn. J. Appl. Phys. **30**. 2159 (1991).

- [7] Y. Ishibashi and H. Orihara, *J. Phys. Soc. Jpn.* **61**. No. 12, 4650-4656 (1992).
- [8] E. Tokumitsu, N. Tanisake and H. Ishiwara, *Jpn J. Appl. Phys.* **33**. 5201-5206 (1994).
- [9] C. L. Wang and S. R. P. Smith, *J. Phys.: Condens. Matter* **8**. 4813-4822 (1996).
- [10] R. E. Cohen, *J. Phys. Chem. Solids* **61**. 139 (2000)
- [11] M. C. Wang, F. Y. Hsao, C. S. His, and N. C. Wu, *J. Crystal Growth*, **246**. 78-84 (2002).
- [12] Y. ISHIBASHI, M. IWATA and A. M. A. Masleh, submitted to *J. Phys. Soc. Jpn.* (2007).
- [13] K. H. Chew, J. Osman, R. L. Stamps, D. R. Tilley, F. G. Shin, and H. L. W. Chan, *J. Appl. Phys.* **93**. 4215 (2003)
- [14] P. C. Ooi, Y. Ishibashi, S. C. Lim, and J. Osman, *Ferroelrc.* **335**. (2007)
- [15] T. Katayama, M. Shimizu, and T. Shiosaki, *Jpn. J. Appl. Phys.* **32**, 3943 (1993)
- [16] L. H. Ong, J. Osman, and D. R. Tilley, *Phys. Rev. B*, **63**, 144109 (2001)

#### **Acknowledgements**

The work is funded by the SAGA grant, Academy of Sciences Malaysia (Grant No: 304/PFIZIK/653018/A118).

## Figure Captions

Fig.1 Polarization profiles during switching, at various time in term of fraction of the switching time  $\tau_s$ , at temperature  $t = 0.5$ , applied field  $e = 0.3$  for thicknesses: (a)  $l = 4.5$ ; (b)  $l = 10.0$ ; (c)  $l = 15.0$  for fixed surface boundary condition. The number at each curve represents time taken to reach the stage in term of fraction of  $\tau_s$ .

Fig.2 Polarization profiles during switching, at various time in term of fraction of the switching time  $\tau_s$ , at temperature  $t = 0.5$ , applied field  $e = 0.3$  for thicknesses: (a)  $l = 4.5$ ; (b)  $l = 10.0$  for free surface boundary condition. The number at each curve represents time taken to reach the stage in term of fraction of

Fig. 3 Polarization current versus time for: a) current central site (dashed line); b) average current (solid line); c) surface site (dotted line); at temperature  $t = 0.5$ , applied field  $e = 0.3$  and  $l = 10.0$ .

Fig. 4 Variation of coercive field  $e_{cf}$  versus film thickness  $l$  for fixed and free surface boundary conditions; in the case of free surface boundary, curves for two values of  $\delta$  are shown.

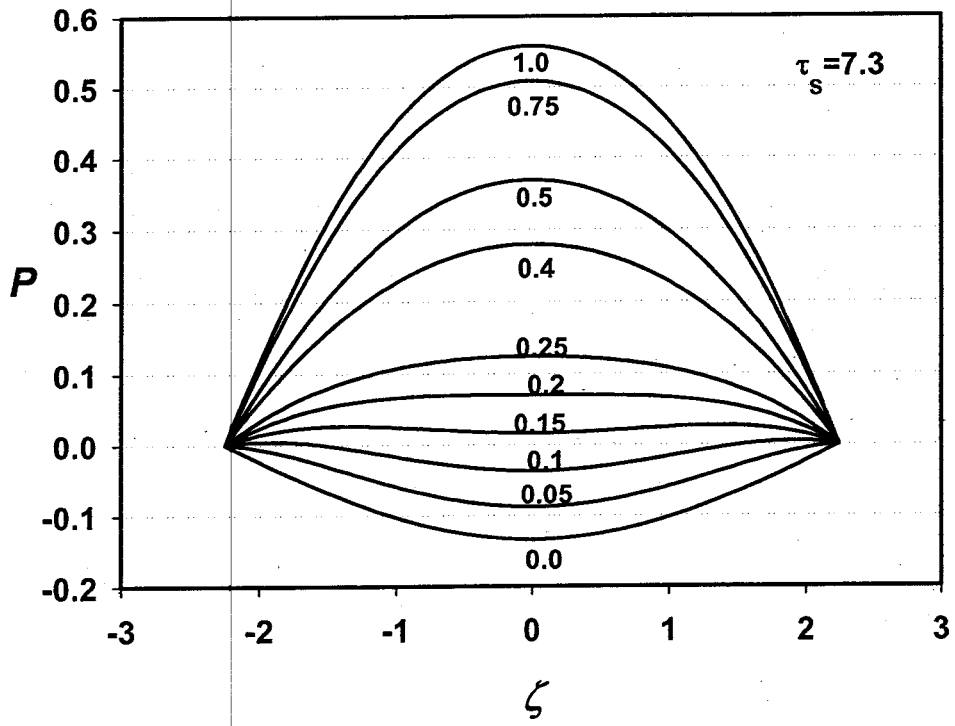


Fig 1 (a)

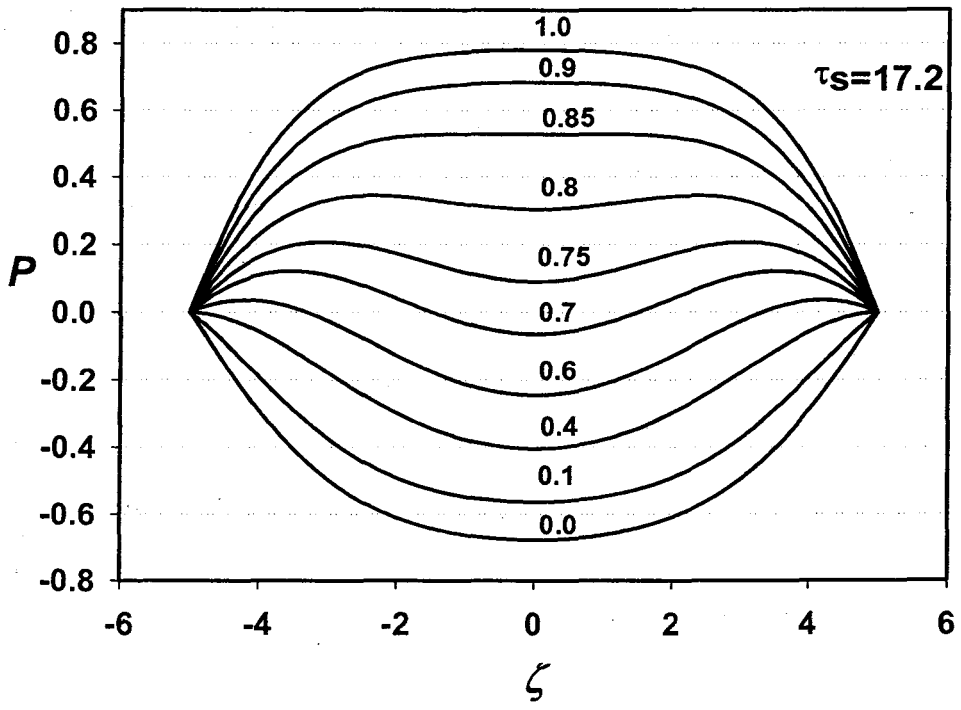


Fig. 1 (b)

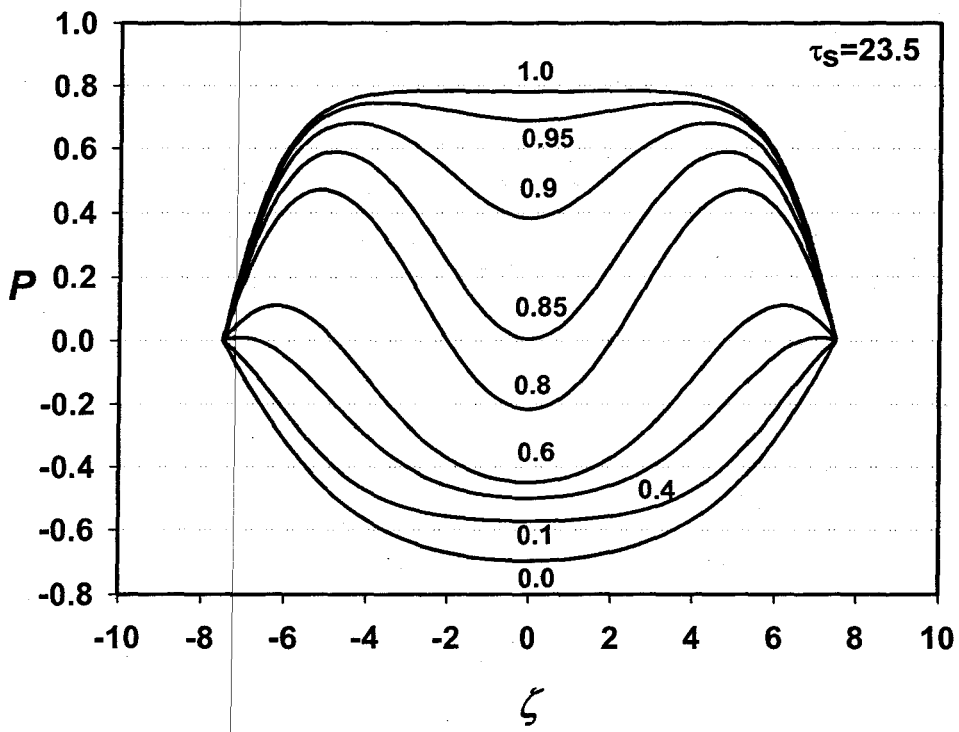


Fig. 1 (c)

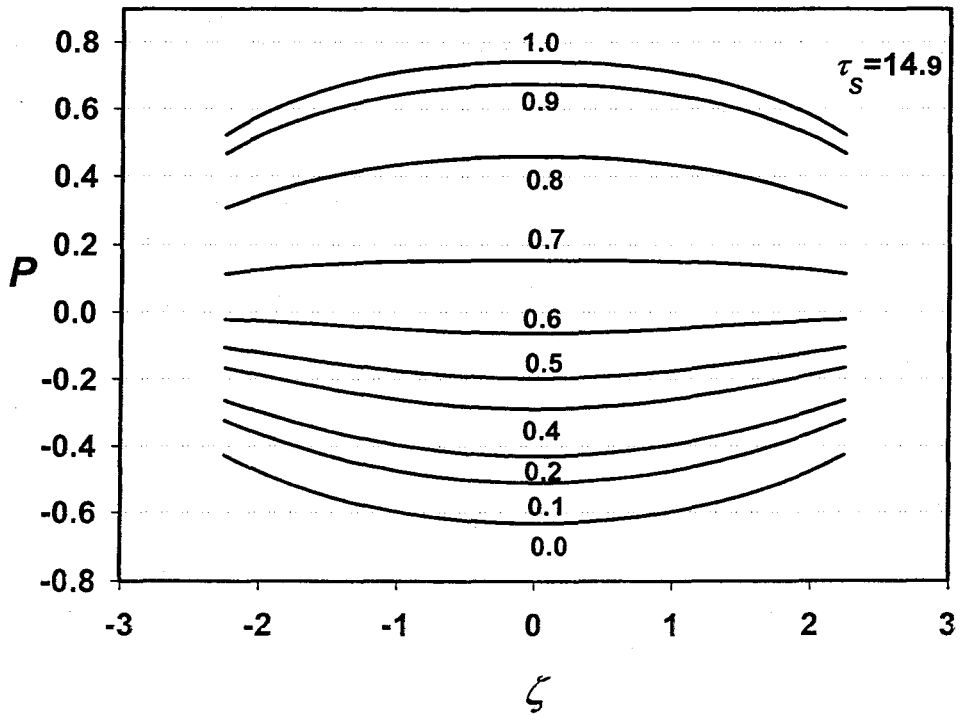


Fig. 2 (a)

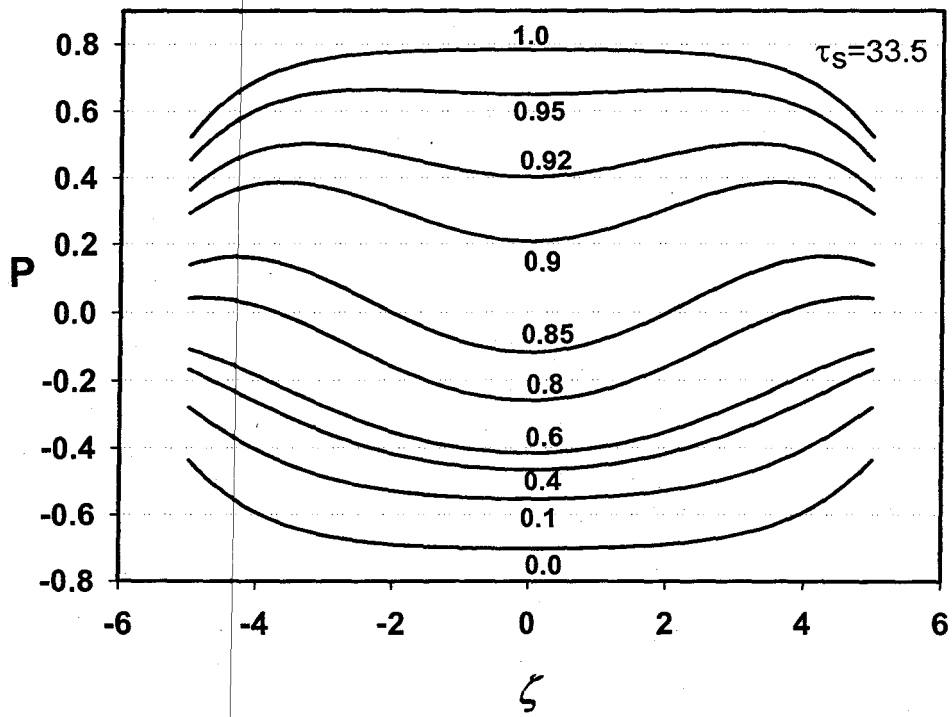


Fig. 2 (b)

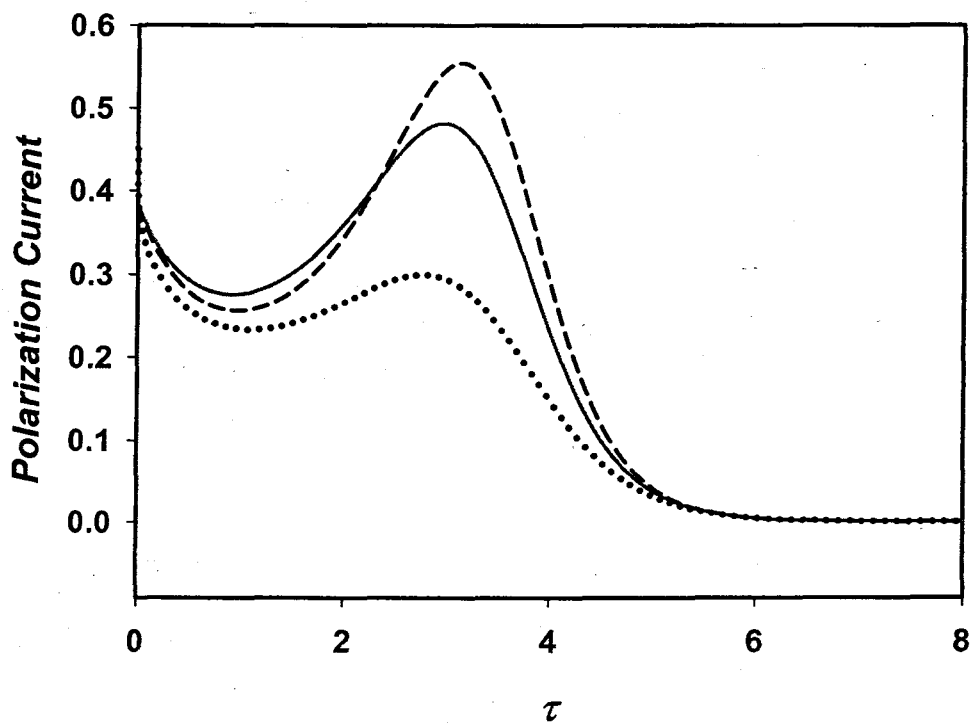


Fig. 3.

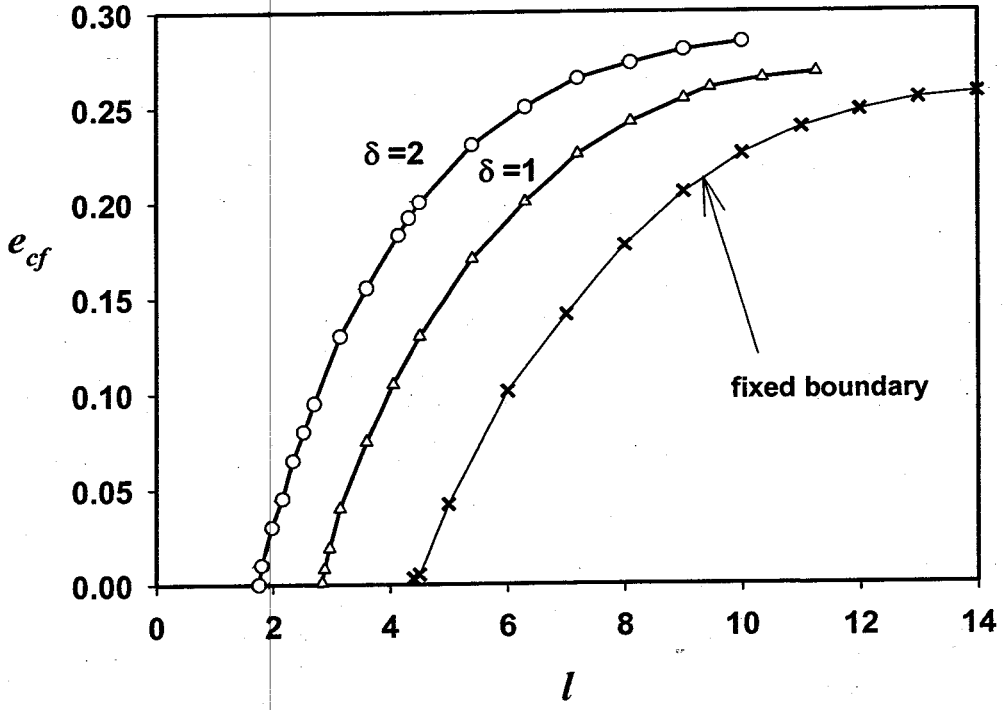


Fig. 4